PB81-164634

Development of an Air Quality Dispersion Model for Aluminum Reduction Plants

Environmental Research and Technology, Inc.
Concord, MA

Prepared for

Environmental Protection Agency
Washington, DC

Aug 80

U.S. Department of Commerce
National Technical Information Service
NTIS

Document P-7304A
August 1980

PB81-164634

Prepared for
The Aluminum Association, Inc.
818 Connecticut Avenue, NW
Washington, DC 20006

Development of an air quality dispersion model for aluminum reduction plants

Prepared by

Lloyd L. Schulman
Project Director

Joseph S. Scire
Principal Investigator

ERT
ENVIRONMENTAL RESEARCH & TECHNOLOGY, INC.
CONCORD, MA • LOS ANGELES • ATLANTA • PITTSBURGH
FORT COLLINS, CO • BILLINGS, MT • HOUSTON • CHICAGO

REPRODUCED BY
NATIONAL TECHNICAL
INFORMATION SERVICE
U.S. DEPARTMENT OF COMMERCE
SPRINGFIELD, VA. 22161

NOTICE

THIS DOCUMENT HAS BEEN REPRODUCED FROM THE BEST COPY FURNISHED US BY THE SPONSORING AGENCY. ALTHOUGH IT IS RECOGNIZED THAT CERTAIN PORTIONS ARE ILLEGIBLE, IT IS BEING RELEASED IN THE INTEREST OF MAKING AVAILABLE AS MUCH INFORMATION AS POSSIBLE.

30272-101

REPORT DOCUMENTATION PAGE	1. REPORT NO. EPA/DF-81-001c	2.	3. Recipient's Accession No. PB81 164634
4. Title and Subtitle	Development of an air quality dispersion model for aluminum reduction plants		5. Report Date August 1980
			6.
7. Author(s)	Lloyd L. Schulman and Joseph S. Scire		8. Performing Organization Rept. No. P-7304A
9. Performing Organization Name and Address	Environmental Research and Technology, Inc. 696 Virginia Road Concord, MA 01742		10. Project/Task/Work Unit No. 11. Contract(C) or Grant(G) No. (C) (G)
12. Sponsoring Organization Name and Address	The Aluminum Association, Inc. 818 Connecticut Avenue, NW Washington, DC 20006		13. Type of Report & Period Covered final, through Aug 80 14.

15. Supplementary Notes

For magnetic tape see PB81 164600

16. Abstract (Limit: 200 words)

An air quality dispersion model, BLP, was developed to simulate the transport and diffusion of effluents from aluminum reduction plants. These plants are complex emission configurations consisting of multiple parallel low-level buoyant line sources interspersed, in most cases, by short point sources. Available air quality models do not adequately describe the dispersion of effluents from aluminum reduction plants or other geometrically similar facilities.

A wind tunnel simulation program of two aluminum reduction plants and an SF_6 field tracer program at one of these plants was used to obtain data for the development of the model.

The model determines plume rise from buoyant line sources and analytically incorporates the effects of multiple lines, wind direction, vertical wind speed shear, and downwash. Plume rise from buoyant point sources also incorporates the effects of vertical wind speed shear and downwash.

The model was verified using two years of SO_2 measurements at the second plant simulated in the wind tunnel program and the results of the SF_6 field tracer program.

17. Document Analysis a. Descriptors

Atmospheric pollution
Air pollution
Algorithms
Diffusion
models
simulation
meteorology

b. Identifiers/Open-Ended Terms

Air Quality Simulation Models (AQSM)
Air Pollutant Dispersion Models

c. COSATI Field/Group 04 02 Atmospheric Sciences/Meteorology

18. Availability Statement	19. Security Class (This Report)	21. No. of Pages
Release Unlimited	UNCLASSIFIED	
	20. Security Class (This Page) UNCLASSIFIED	22. Price

ABSTRACT

An air quality dispersion model was developed to simulate the transport and diffusion of effluents from aluminum reduction plants. These plants are complex emission configurations consisting of multiple parallel low-level buoyant line sources interspersed, in most cases, by short point sources. Available air quality models do not adequately describe the dispersion of effluents from aluminum reduction plants or other geometrically similar facilities.

A wind tunnel simulation program of two aluminum reduction plants and an SF_6 field tracer program at one of these plants was used to obtain data for the development of the model.

The model determines plume rise from buoyant line sources and analytically incorporates the effects of multiple lines, wind direction, vertical wind speed shear, and downwash. Plume rise from buoyant point sources also incorporates the effects of vertical wind speed shear and downwash.

The model was verified using two years of SO_2 measurements at the second plant simulated in the wind tunnel program and the results of the SF_6 field tracer program.

Preceding page blank

ACKNOWLEDGEMENTS

Many people contributed to the success of this program. Valuable assistance was provided by the Aluminum Association Inc., represented by Seymour G. Epstein, Lawrence C. Tropea, Dr. Patrick R. Atkins, William J. Janson, John R. Suitlas, and Kenneth N. Weiss. Guidance and advice was also provided by D. Bruce Turner, who represented EPA on the program. The authors would also like to acknowledge the ERT personnel, principally Dr. Peter J. Drivas in the field program, Carl W. Benkley in the wind tunnel program, and Dr. James R. Mahoney for their contributions to the model development program.

Preceding page blank

TABLE OF CONTENTS

	Page
ABSTRACT	iii
ACKNOWLEDGEMENTS	v
1. INTRODUCTION	1-1
2. DATA COLLECTION PROGRAMS	2-1
2.1 Wind Tunnel Program	2-1
2.2 Field Study Tracer Program	2-2
3. MODEL DEVELOPMENT	3-1
4. MODEL PERFORMANCE EVALUATION	4-1
4.1 Comparison of Model Results with Field Study Tracer Data	4-1
4.2 Comparison with Measured SO_2 Data	4-15
4.2.1 Meteorological Data	4-15
4.2.2 Emissions Data	4-16
4.2.3 Air Quality Data	4-21
4.2.4 Evaluation Results	4-21
5. SUMMARY AND CONCLUSIONS	5-1
REFERENCES	
APPENDIX HOURLY FIELD STUDY SF_6 DATA	

Preceding page blank

1. INTRODUCTION

Environmental Research & Technology, Inc. (ERT) was retained by The Aluminum Association, Inc. to develop an air quality dispersion model to simulate the transport and diffusion of emissions from aluminum reduction plants. These facilities are complex areal emission sources composed of continuous low-level buoyant line sources called potrooms and, in most cases, low-level stack releases. The dispersion of these effluents, especially from the buoyant line sources, are not correctly described by currently available air quality models.

Alumina is reduced through electrolysis to aluminum in the potrooms. A reduction facility typically consists of 2 to 20 potroom buildings, approximately 500 meters long. Some of the buoyant emissions from the reduction process escape through a continuous ridge ventilator, a few meters wide, running the length of the potroom. Most of the emissions, however, are collected by hooding above the reduction cells and are treated and exhausted through nearby stacks. There are typically 2 to 20 point sources, usually low level, for each potroom primary control system.

Because of the complex emission configuration of an aluminum reduction plant, an ambitious data collection program was undertaken to obtain sufficient information to develop the model. After completion of the model, additional data were used to evaluate model performance. The program was divided into four phases.

1) A wind tunnel simulation program was conducted using physical models of two existing reduction plants. Approximately 50 experiments were performed to study plume rise, plume dispersion, and the effects of wind speed and wind direction on plant emissions.
2) A field study tracer program was conducted at one of the two plants modeled in the wind tunnel program. To simulate the line source, SF_6 was released from 3 points on a potroom building and 28 hourly averaged measurements were made

during five experiments. Concurrent meteorological soundings were made between 10 and 50 meters above the ground from a tethersonde system.

3) The air quality dispersion model, Buoyant Line and Point source (BLP), was developed based on the data from the wind tunnel and field study programs, new line and point source plume rise theory, and diffusion modeling concepts.

4) The model was verified using both the SF_6 tracer measurements from the field program, and two years of SO_2 measurements at a monitor 300 meters east of the second plant simulated in the wind tunnel program.

This report briefly reviews the first three phases of the model devlopment project, since extensive documentation of these activities already exists (Hoydysh, Estrada, and Perry 1979; Klauber and Mazaika 1979; and Schulman and Scire 1980). The wind tunnel and field study programs are briefly described in Section 2, and the model development in Section 3. A more detailed evaluation of the model performance and subsequent verification is presented in Section 4. A summary of the project is presented in Section 5.

2. DATA COLLECTION PROGRAMS

The data collection necessary to develop the BLP model consisted of a wind tunnel simulation program for two aluminum reduction plants and SF_6 field tracer program at one of those plants. This section reviews these data gathering programs and reports on the key results.

2.1 Wind Tunnel Program

A wind tunnel testing program was conducted to determine near-field plume rise and plume dispersion characteristics for the potroom and the scrubber exhaust stack emissions. Separate modeling simulations were conducted for both the Reynolds Metals Company's (RMC) Patterson Reduction Plant in Arkadelphia, Arkansas, and the Aluminum Company of America (Alcoa) Tennessee South Reduction Plant in Alcoa, Tennessee. The details of the wind tunnel program have been reported by Hoydysh, Estrada, and Perry (1979) and are summarized below.

The wind tunnel program investigated the effects of both wind speed and direction on plume rise and downwind concentration measurements for each of the plants. Concentration measurements along horizontal and vertical profiles at several downwind distances were made at up to 30 sampling points. Three wind speeds and three wind directions (perpendicular, parallel, and 45°) were used in the tests. Besides the vertical concentration measurements, plume rise could be estimated from photographs of a buoyant oil fog released from the emission sources. In addition to the concentration measurements and plume photographs, flow visualization photographs were taken of neutrally buoyant helium bubbles and upwind velocity and turbulence profile were obtained for each of the three wind directions. In all, 49 tests were performed.

The two reduction plants were both modeled to evaluate the effects on plume dispersion of different plant size and scrubber exhaust stack heights. The RMC Patterson plant consists of only 2 potrooms with 4 tall scrubber stacks. The Alcoa Tennessee plant has four potrooms and 48 short scrubber stacks, which are approximately the same height as the potrooms.

Because of its larger size, the Alcoa plant produces more heat. Nine tests were conducted that simulated heat loss by means other than convection of exhaust gases through the potroom ridge ventilators and scrubber stacks. This was accomplished by attaching resistance heating strips to the potroom buildings.

Despite the plant size difference, the behavior of the buoyant line source emissions from the potrooms was similar for both the RMC Patterson and Alcoa Tennessee plants. At all wind speeds (the lowest tested was approximately 4 meters per second) the plume was immediately downwashed to the ground (the potroom height is typically 15 to 20 meters), but subsequently rose. Under the lightest wind speeds, the plume actually lifted off the ground at about 1 kilometer downwind. At the higher wind speeds, no lift-off was observed. Lift-off occurs when the downwind increase in plume height is larger than the vertical plume growth.

Line source plume rise was larger for parallel winds than for perpendicular or 45° wind directions. Under parallel wind conditions, the buoyant line elements merge as they advect over the length of the line and the plume rise is enhanced.

As expected, the behavior of the scrubber stack plumes was quite different for the two plants. For the taller stacks at the RMC plant (about 2.3 times the potroom height), there was no effect of the buildings on plume rise or dispersion. At the Alcoa plant, however, the short scrubber stacks were strongly downwashed over the range of wind speeds tested.

The nine building heat loss tests showed only very small differences from the tests without building heating. Apparently, at least for the range of wind speeds tested, the air flow over the plant is not significantly modified by the heated building surfaces nor is the buoyancy of the source emissions significantly increased.

2.2 Field Study Tracer Program

An SF_6 tracer program was conducted at the RMC Patterson Reduction Plant to study the dispersion of effluents from the potrooms. The RMC plant was chosen because its small size,

and the surrounding rural, open countryside made the logistics of a field experiment simpler. A detailed description of the tracer program and the results has been reported by Klauber and Mazaika (1979).

At three points along the approximately 550 meter roof, SF_6 was injected into the potroom line source. The points were sufficiently close to simulate a line source release at several hundred meters downwind. Hourly averaged samples of ambient air were gathered from a network of 19 programmable bag samplers and were analyzed for SF_6 content. The samplers were located along three arcs at 750, 1,500, and 2,250 meters downwind. One sampler was located approximately 100 meters downwind to detect downwash contributions, and one sampler was located upwind to measure background concentrations.

In addition to the tracer release and sampling network, meteorological measurements were made through about a 50-meter depth of the atmosphere upwind of the plant using a tethersonde system. Wind speed and direction, temperature, wet bulb temperature, and pressure were measured as the tethered balloon was alternately raised and lowered during each experiment.

Five separate experiments over two weeks were conducted, and 28 hours of data were collected. The meteorological conditions ranged from light wind speeds and slightly unstable or neutral stability to high wind speeds and neutral stability. Under even the lightest wind speeds, the highest concentrations were measured at the sampler 100 meters downwind of the plant, indicating that downwash of the potroom plume was important. This result agreed with the smoke tracer observations in the wind tunnel showing plume downwash at the lowest speeds tested. Another key observation in the field experiment was that the plume lifted off after the initial downwash. The distance to lift-off increased with increasing wind speed. This feature was also observed in the wind tunnel.

3. MODEL DEVELOPMENT

The results of the wind tunnel tests and SF_6 field experiment described in Section 2 indicated that there are many special considerations in modeling aluminum reduction facilities. The special modeling problems associated with multiple low-level buoyant line and point sources necessitated that new modeling techniques be developed to correctly describe the dispersion of effluents from these complex sources. These developments summarized below are discussed in detail in the Buoyant Line and Point Source (BLP) Dispersion Model User's Guide (Schulman and Scire 1980).

A literature search was initiated to uncover plume rise research applicable to the problems of multiple line source rise, wind shear, and building downwash. Plume rise from tall, buoyant point sources has been extensively studied and is well represented by the plume rise equations of Briggs (1969, 1970, 1975). The plume rise from low-level point sources, however, can be significantly affected by vertical wind shear and building downwash. Using the Briggs equations, which do not include shear and downwash effects, can lead to overestimated effective stack height predictions for low-level sources. Sheih (1978) compared predicted pollutant concentrations using a conventional diffusion model with no wind shear and a numerical diffusion model incorporating wind shear. It was found that neglecting wind shear led to errors up to a factor of two in the predicted concentration. The building downwash wind tunnel tests of Huber and Snyder (1976) indicated plume rise was reduced one third by the presence of a building as compared to the plume rise from an isolated stack. The BLP model uses plume rise equations especially developed to analytically incorporate the effects of vertical wind shear and building downwash. Importantly, these equations reduce to the Briggs plume rise equations in the special case of no vertical wind shear or building downwash.

The rise of the buoyant line source (potroom) effluent cannot be correctly determined by the conventional point-source plume rise equations. Briggs (1977), using TVA data, proposed an empirical enhancement factor for multiple point souces. Murphy (1975) and Anfossi et al. (1978) presented enhancement schemes for multiple point sources using virtual source techniques. None of these schemes, however, incorporated the effects of building downwash and vertical wind shear. To correctly describe the plume rise from aluminum reduction facility potrooms, the plume rise enhancement associated with the merging of the plumes from multiple potrooms, the wind direction dependence characteristic of plume rise of a buoyant line source, as well as building downwash and vertical wind shear effects must be considered. A set of line source plume rise equations were developed for the BLP model to analytically incorporate all these effects. These line source plume rise equations will reduce to the Briggs point source plume rise equations as the line source length approaches zero for the special case of no vertical wind shear or building downwash.

The major features of the BLP dispersion model are illustrated in Table 3-1. In addition to the plume rise developments, the BLP model includes pollutant decay, terrain adjustment, and enhanced building downwash dispersion coefficients (using a virtual source approach). The post-processing program, POSTBLP, allows flexible manipulation of the source contribution or total concentration files. The capabilities of the POSTBLP program are outlined in Table 3-2. A complete technical description of the BLP model and user's instructions for both the BLP and POSTBLP programs are included in the Buoyant Line and Point Source (BLP) Dispersion Model User's Guide (Schulman and Scire 1980).

TABLE 3-1

MAJOR FEATURES OF THE BLP MODEL

- UTM or line source oriented (SCS) coordinate systems.
- Multiple point source and finite buoyant line source capability.
- Finite buoyant line source plume rise.
- Plume enhancement due to multiple line sources.
- Vertical wind shear in plume rise formulations for both point and line sources.
- Transitional plume rise.
- Incorporation of building downwash in both dispersion and plume rise calculations for point and line sources.
- Terrain adjustment plume path coefficients.
- Time-dependent pollutant decay.
- Source contribution concentrations.
- Flexible post-processing package.

TABLE 3-2

MAJOR FEATURES OF THE POSTBLP PROGRAM

- Total concentration or source contribution analysis.
- Monthly and annual frequency distributions for 1-, 3-, and 24-hour average concentrations.
- Tables of 1-, 3-, and 24-hour average concentrations at each receptor.
- Table of the annual (or length of the BLP run) average concentrations at each receptor.
- Five highest 1-, 3-, and 24-hour average concentrations at each receptor.
- Fifty highest 1-, 3-, and 24-hour average concentrations in the receptor field.

TABLE 4-1

METEOROLOGICAL DATA USED IN THE BLP MODEL

TRACER STUDY SIMULATIONS

Date (1979)	Hour	Wind Direction (degrees)	Wind Speed (m/s)	Stability Class (estimated)	Cloud Conditions
March 18	12	161	6.92	D	Overcast, low clouds
	13	159	6.42	D	Overcast, low clouds
	14	177	7.15	D	Scattered clouds
	15	169	5.36	D	Scattered clouds
March 20	10	240	3.20	C	Scattered clouds
	11	248	6.35	D	Scattered clouds
	12	260	6.71	D	Scattered clouds
	13	253	7.02	D	Scattered clouds
March 26	8	75	1.75	B	Scattered clouds
	9	111	1.42	B	Scattered clouds
	10	112	2.67	C	Scattered clouds
	11	159	4.18	D	Scattered clouds
	12	176	5.54	D	Scattered clouds
	13	189	7.33	D	Scattered clouds
	14	181	7.33	D	Scattered clouds
	15	190	7.42	D	Scattered clouds
March 28	12	189	8.76	D	Overcast, low clouds
	13	191	8.05	D	Overcast, low clouds
	14	192	8.76	D	Overcast, low clouds
	15	185	7.87	D	Overcast, low clouds
March 29	10	183	9.12	D	Overcast, low clouds
	11	180	8.31	D	Overcast, low clouds
	12	187	9.39	D	Overcast, low clouds
	13	184	8.94	D	Overcast, low clouds
	14	181	8.76	D	Overcast, low clouds
	15	180	7.60	D	Overcast, low clouds
	16	183	9.39	D	Overcast, low clouds
	17	178	7.33	D	Overcast, low clouds

(15.8 meters). In addition to tethersonde wind speed and wind direction measurements, the data from an on-site fixed anemometer and wind vane were used to develop the hourly averaged wind speeds and wind directions used in the BLP model simulations.

The normalized measured and predicted SF_6 concentrations at each receptor are tabulated in the appendix for each of the 28 hours. The stack height wind speed, u_s, and the SF_6 emission rate per unit line length, q_L, are used as normalized factors. Observed and predicted normalized concentrations are plotted in Figure 4-2 to 4-11 for various wind speeds. It should be noted that even with the lighter wind speeds, the plume immediately downwashes in the building wake region. The plume then lifts off the ground as the rise of the buoyant plume exceeds the plume growth due to dispersion. As the wind speed increases (and plume rise thus decreases), the plume does not lift off the ground until farther downwind. At the highest wind speed presented (9.12 m/s), the plume (as defined by the 5×10^{-4} m^{-1} line) has not lifted off the ground at 3 kilometers downwind.

In many cases, the observed concentration at the downwash sampler (receptor Number 2) was above the saturation value of the sampler instrument of 1,000 parts per trillion (ppt). The reported normalized concentration for these hours, therefore, is a lower bound of the actual value. For example, a normalized concentration of 300^+ indicates that the sampler saturated and the observed normalized concentration is greater than 300×10^{-4} m^{-1}.

The observed and predicted concentration patterns in Figures 4-2 to 4-11 compare very well over the entire range of wind speed conditions. At the lower wind speeds, the predicted concentration patterns show the same downwash and plume lift-off behavior as the observed concentration patterns; the plume immediately downwashes, leading to the highest concentrations in the near field. With the relatively light wind speeds, buoyant plume rise quickly exceeds the vertical growth of the plume and the normalized concentration decreases rapidly with distance. For the higher wind speeds, the predicted normalized ground-level concentration patterns also closely follow the observed pattern. With the higher wind speeds, the buoyant rise of the plume is reduced resulting in higher normalized

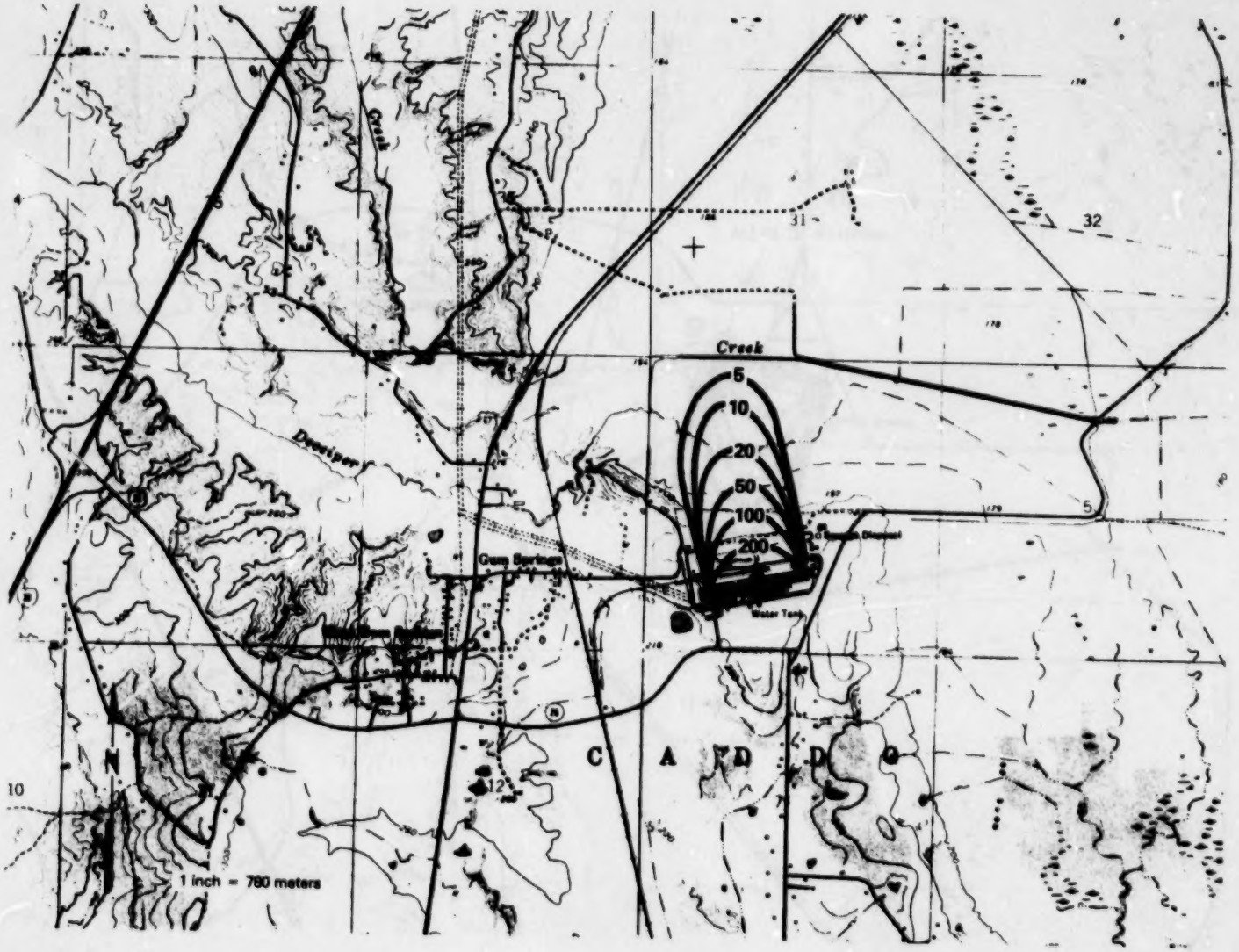

Figure 4-2 Observed $\chi u/q_\ell$ x 10^4 m^{-1} for March 26, 1979 - Hour 11

ENVIRONMENTAL RESEARCH & TECHNOLOGY INC.

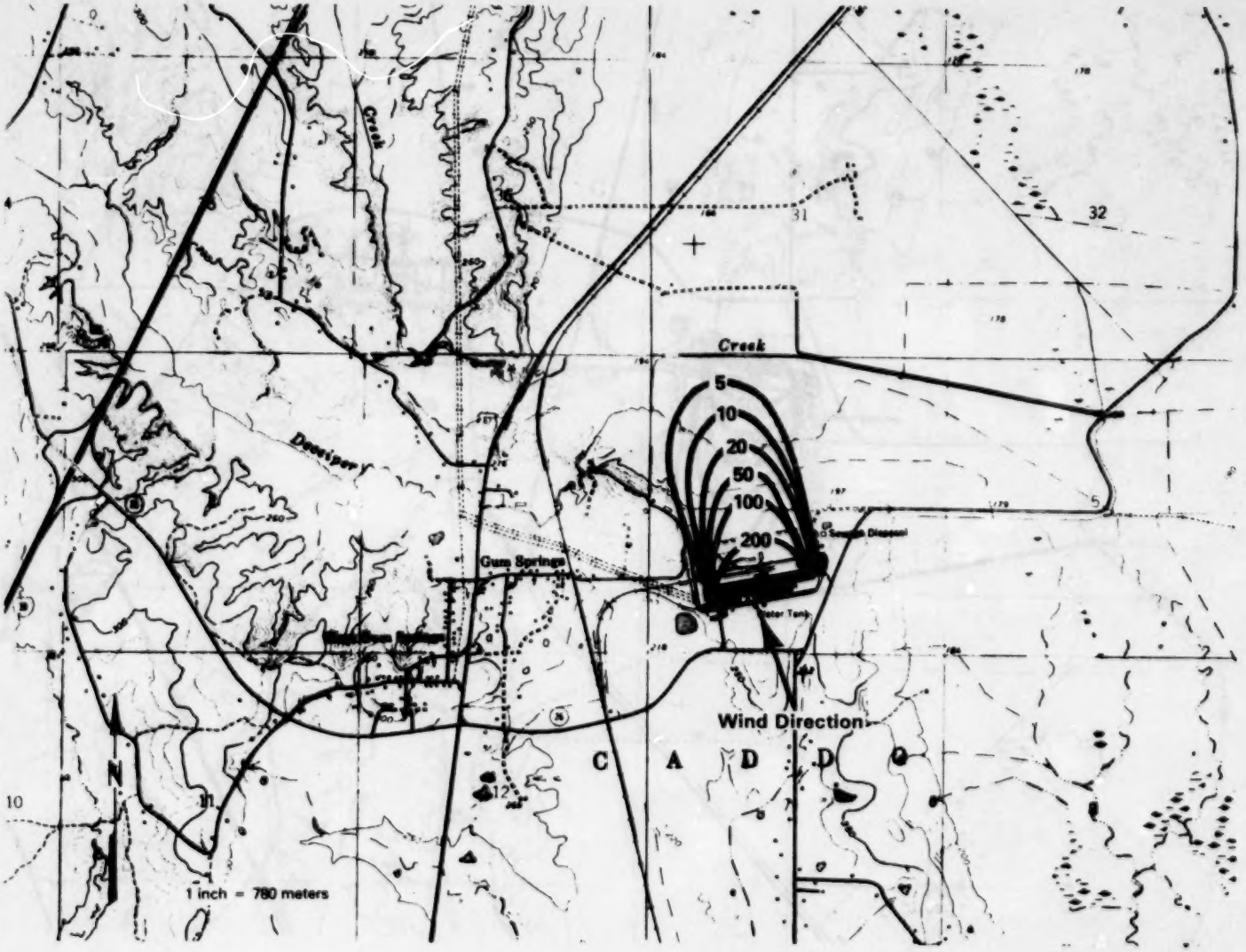

Figure 4-3 Predicted $\chi u/q_\ell$ x 10^4 m^{-1} for March 26, 1979 - Hour 11
(u = 4.18 m/s, θ = 339°)

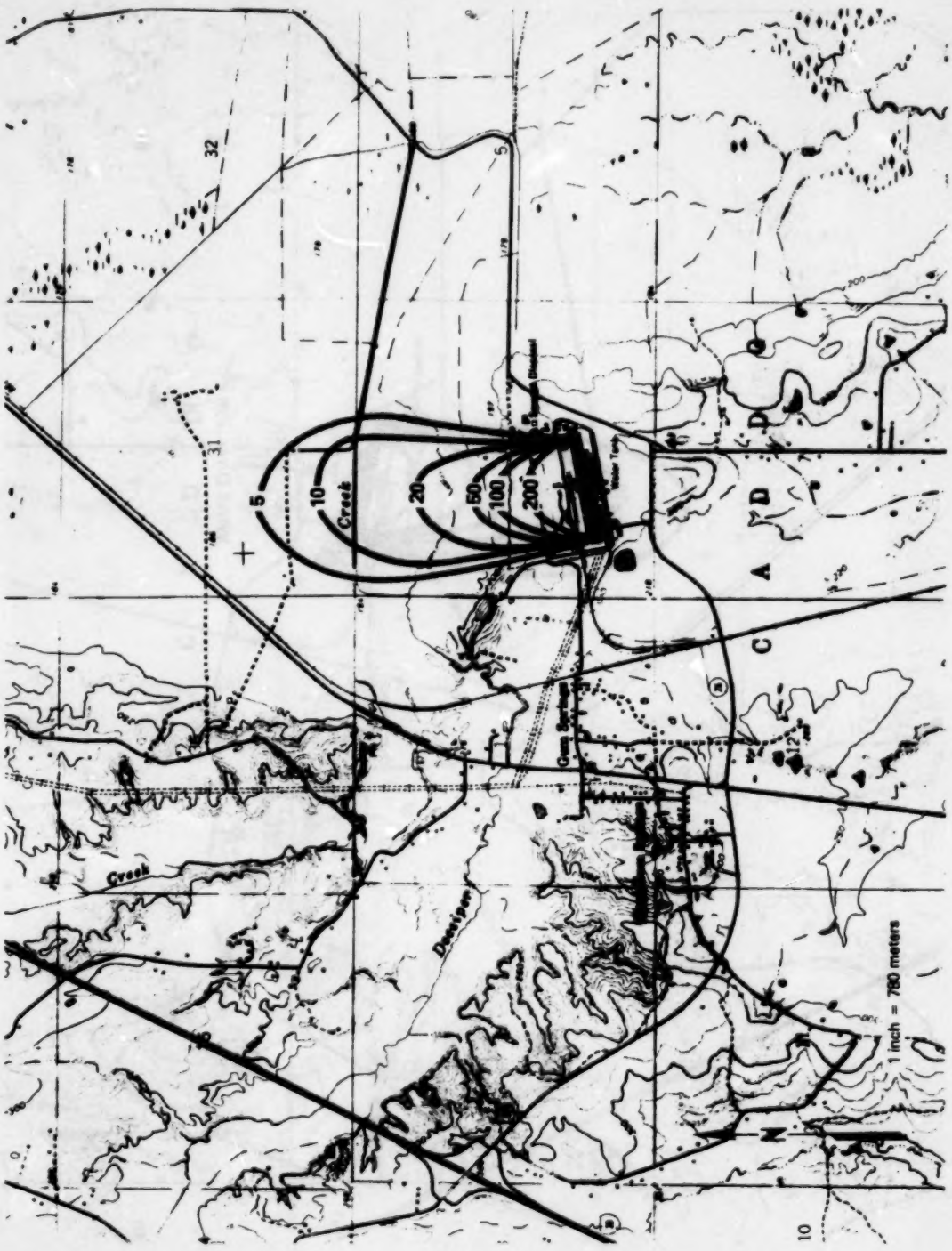

Figure 4-4 Observed $\chi u/q_\ell$ x 10^4 m^{-1} for March 26, 1979 - Hour 12

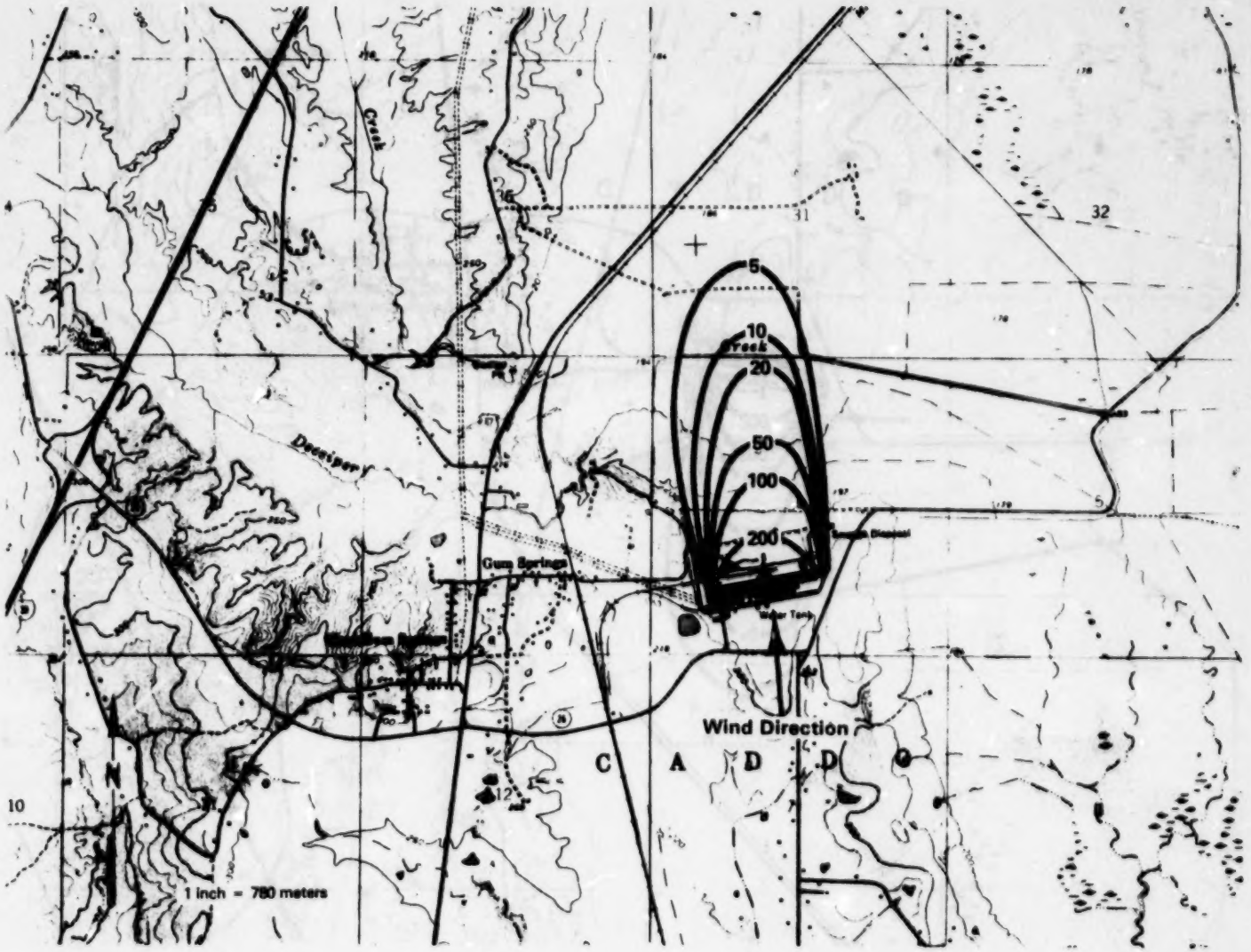

Figure 4-5 Predicted $\chi u/q_\ell$ x 10^4 m^{-1} for March 26, 1979 - Hour 12
(u = 5.54 m/s, θ = 356°)

ENVIRONMENTAL RESEARCH & TECHNOLOGY INC.

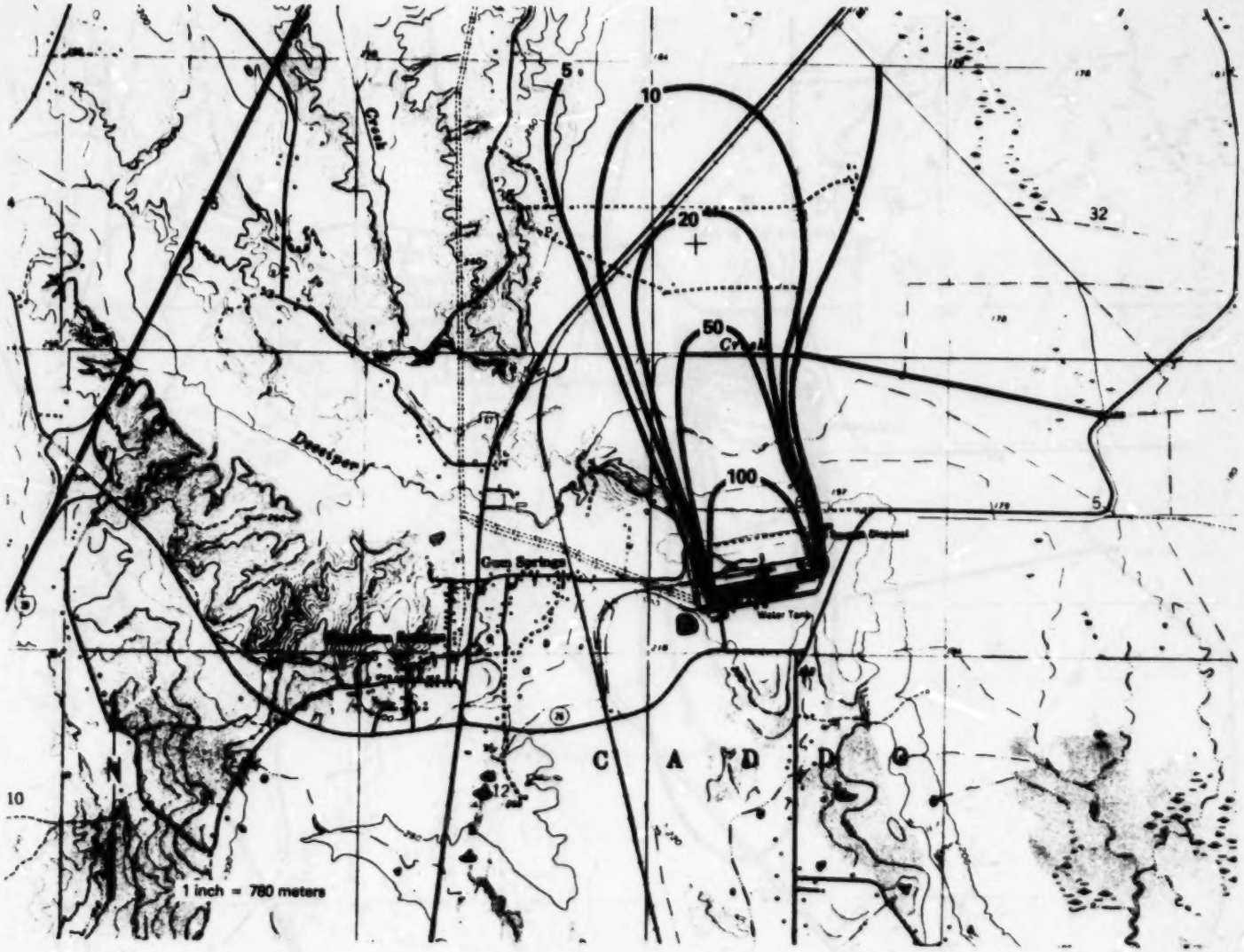

Figure 4-6 Observed $\chi u/q_\ell$ x 10^4 m^{-1} for March 18, 1979 - Hour 14

ENVIRONMENTAL RESEARCH & TECHNOLOGY INC

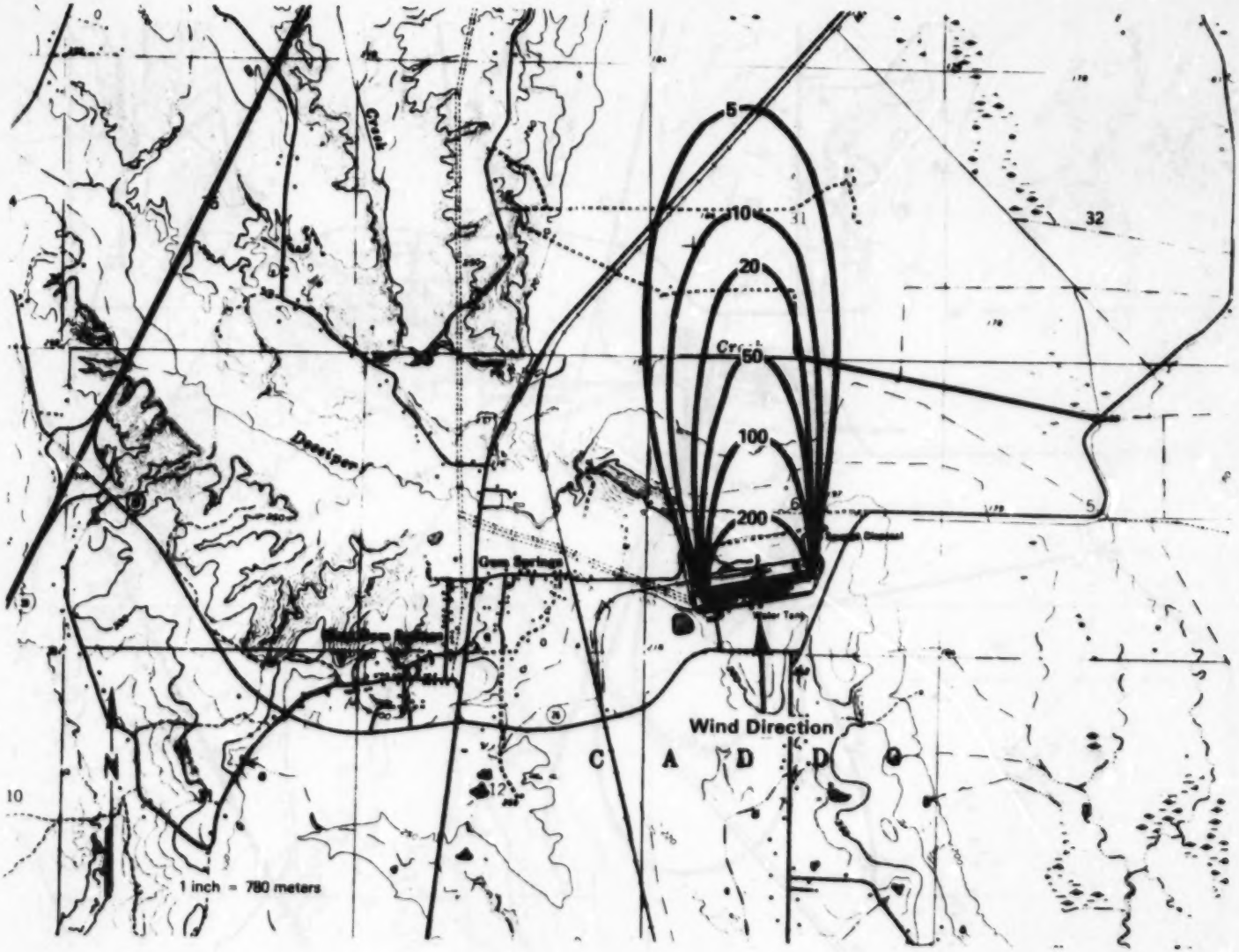

Figure 4-7 Predicted $\chi u/q_\ell$ x 10^4 m^{-1} for March 18, 1979 - Hour 14
(u = 7.15 m/s, θ = 357°)

ENVIRONMENTAL RESEARCH & TECHNOLOGY, INC.

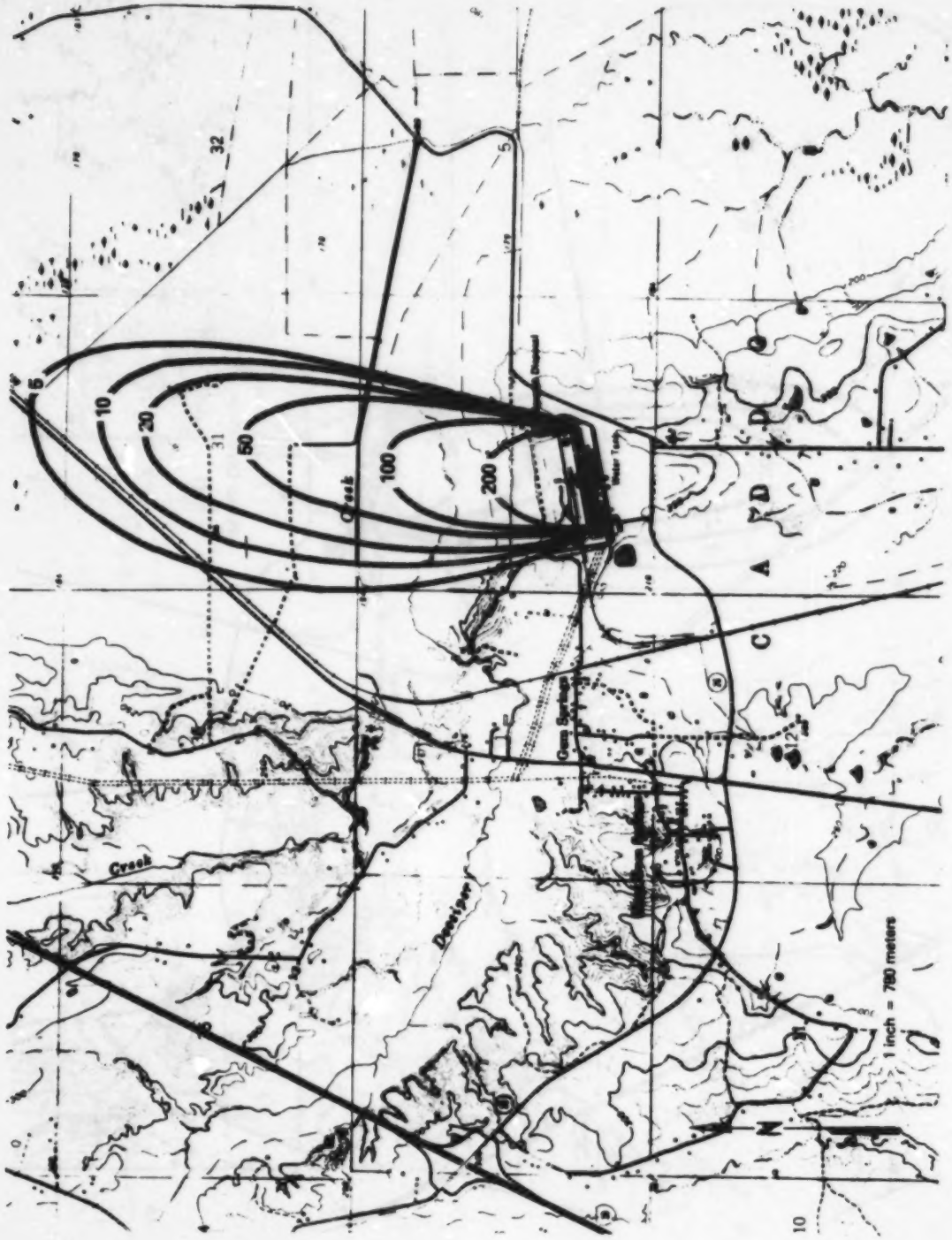
5
10
20
50
100
200
32
31
Creek
Creek
Dry Gulch
Water Tank
Dry Gulch
Dry Gulch
Dry Gulch

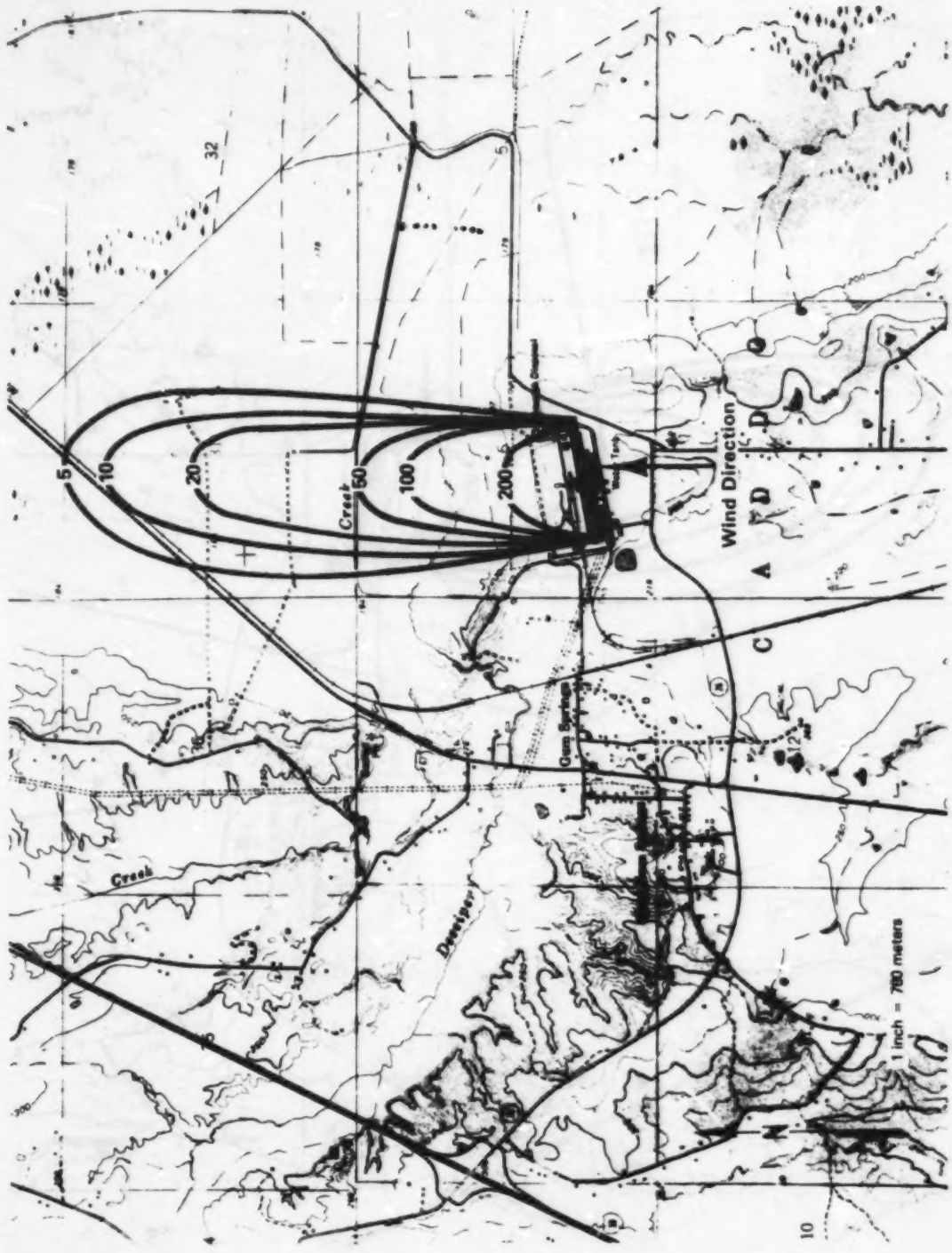

Figure 4-9 Predicted $\chi u/q_\ell$ x 10^4 m^{-1} for March 29, 1979 - Hour 11
(u = 8.31 m/s, θ = 360°)

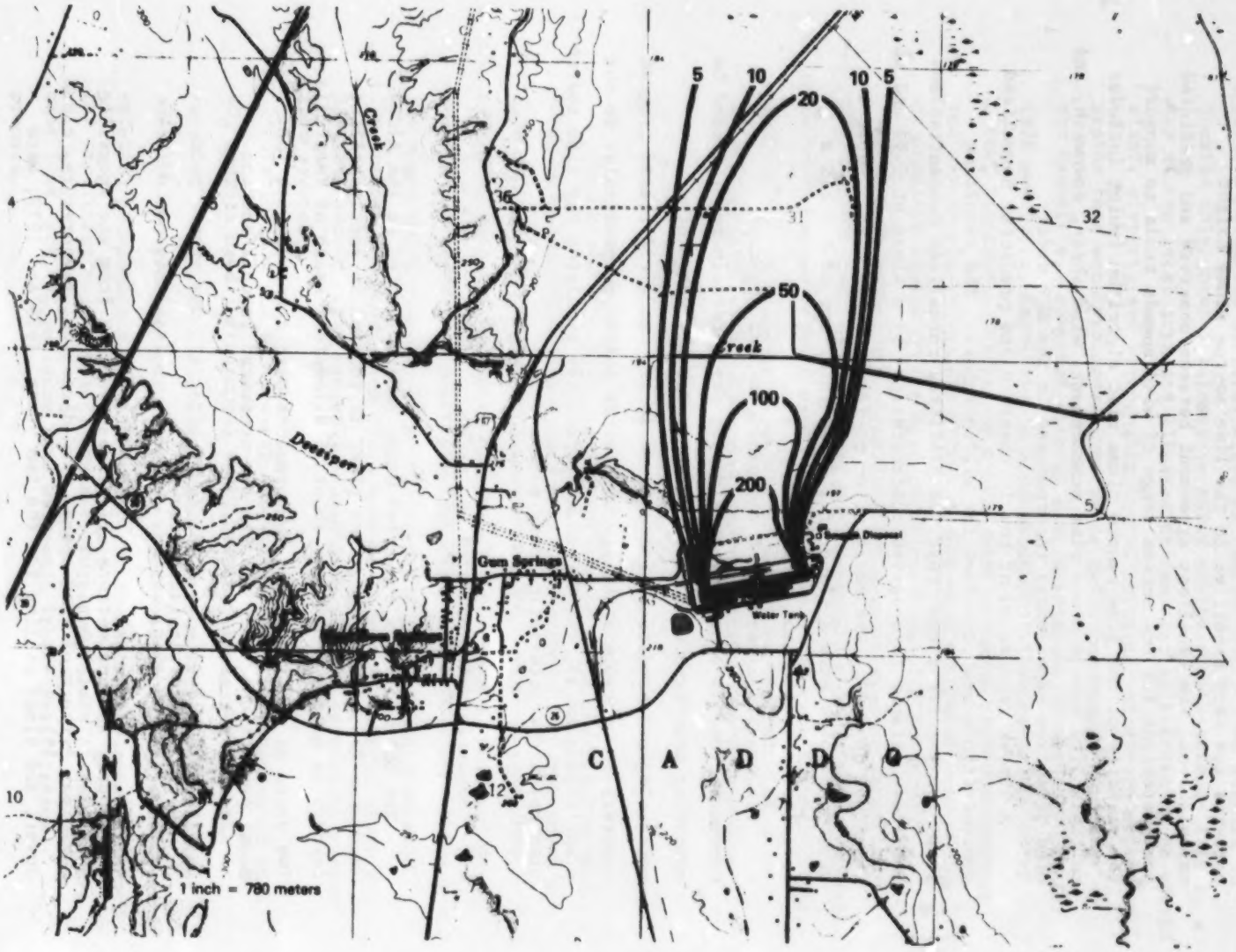

Figure 4-10 Observed $\chi u/q_\ell$ x 10^4 m^{-1} for March 29, 1979 - Hour 10

ENVIRONMENTAL RESEARCH & TECHNOLOGY INC.

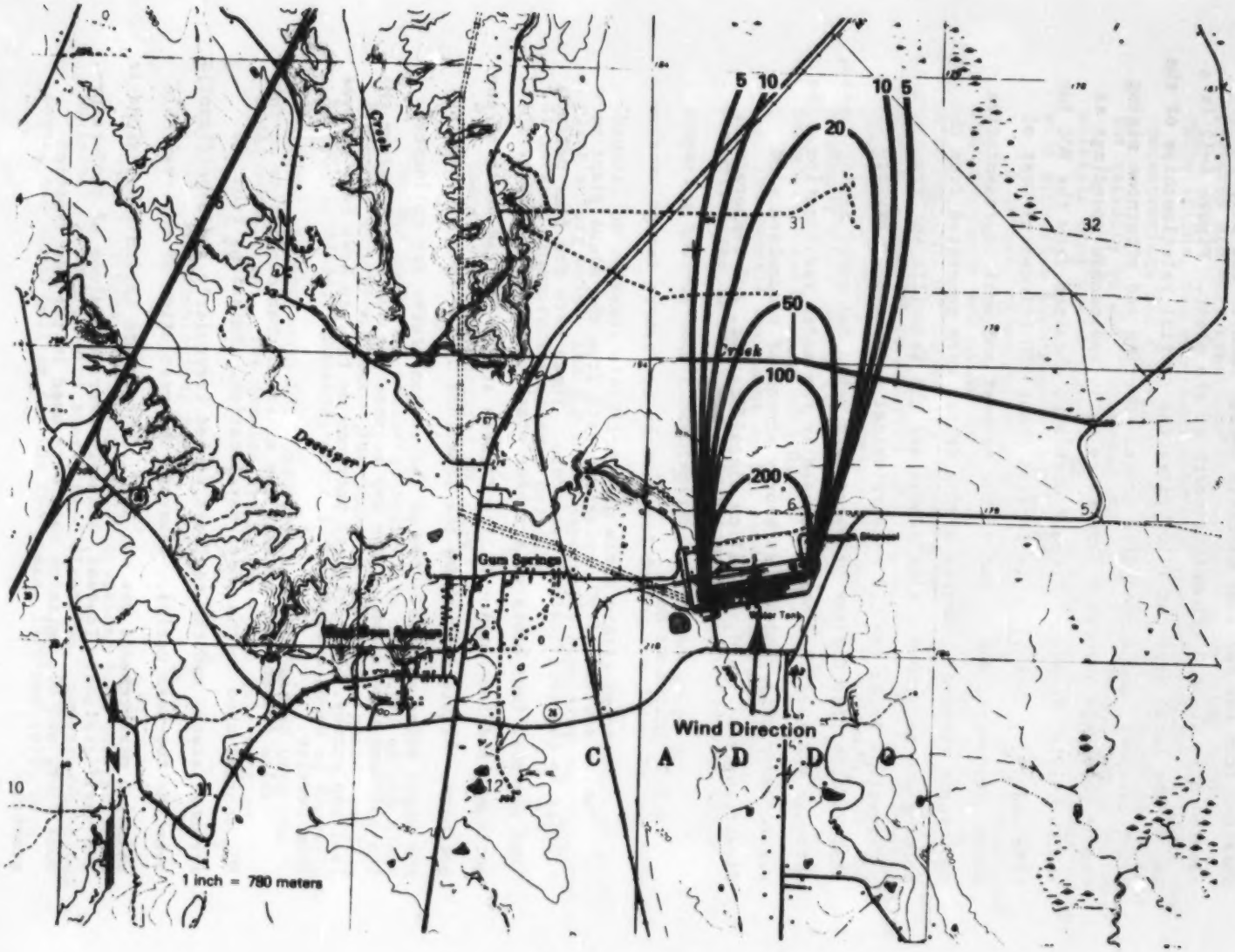

Figure 4-11 Predicted $\chi u/q_\ell$ x 10^4 m^{-1} for March 29, 1979 - Hour 10 (u = 9.12 m/s, θ = 3°)

concentrations farther downwind. Because the predicted concentration patterns are very sensitive to the line source plume height calculations, the excellent agreement between observed and predicted concentrations for the entire range of wind speeds tends to support the validity of the line source plume rise algorithm (which includes multiple line source plume rise enhancement, wind shear, downwash, and wind direction dependency) incorporated in the BLP model.

A linear regression of hourly observed and predicted normalized concentrations was conducted for all receptors. The resulting least-squares fit showed that the predicted normalized concentrations were best related to observed concentrations by a slope of 0.97 and an intercept of 3.27. The correlation coefficient was 0.75. Perfect agreement would have a slope of 1.0, an intercept of 0.0 and a correlation coefficient of 1.0.

The overall agreement of the predicted and observed concentrations is excellent considering the uncertainties involved in comparing hour-by-hour concentrations. For the range of meteorological conditions encountered during the field tracer program (neutral or unstable stability with winds nearly perpendicular to the plant's long axis), the BLP model apparently simulates the line source dispersion characteristics very well.

4.2 Comparison with Measured SO_2 Data

The BLP model was evaluated using data collected at the Alcoa Tennessee Reduction Plant. The plant is located in gently rolling terrain in Alcoa, Tennessee, about 15 kilometers south of Knoxville. Two years of continuous SO_2 measurements were compared with the model predictions. The results are presented in this section.

4.2.1 Meteorological Data

Hourly surface meteorological observations from the Knoxville Municipal Airport of wind speed, wind direction, temperature, cloud cover, and cloud ceiling for the two years, 1976 and 1977, were

obtained from the National Climatic Center (NCC). The airport is located only about 3 kilometers north of the plant. Figure 4-12 is a map of the local area and illustrates the spatial relationships of the plant, airport, and surrounding towns. Morning and afternoon mixing depths that were processed from twice daily radiosonde soundings at the Nashville, Tennessee Airport were also obtained from the NCC for 1976 and 1977. Nashville is located about 250 kilometers west of Alcoa, Tennessee, and is one of the nearest and most representative radiosonde stations. Hourly mixing depths were generated from the morning and afternoon mixing depths and the Knoxville surface observations using the EPA meteorological preprocessor program for CRSTER. The preprocessor produces both urban and rural mixing depths, although the rural heights were used in the model verification. The preprocessor also produces an hourly stream of randomized wind direction, wind speed, stability classification, and temperature.

4.2.2 Emissions Data

Twelve sources of SO_2 emissions data from the Alcoa plant were modeled in the verification procedure. These were the four potroom line sources, four banks of scrubber stacks located in between the potrooms, and four carbon baking furnace stacks located south of the potrooms. Figure 4-13 shows the locations of the four potrooms and the eight point sources. Two of the carbon stacks are collocated. The potrooms were drawn on the map because they were built after the last map survey. The original potrooms on the map have been removed from service.

Tables 4-2 and 4-3 present the emission characteristics of the SO_2 sources used in the model verification. Emissions from the scrubber stacks and the potlines varied irregularly and significantly over the two-year period. However, the resolution of the available emission measurements was not sufficient to use variable emissions in the verificiation. Instead, annually averaged values of temperature, mass flux, and SO_2 emission rate were used in the verification process.

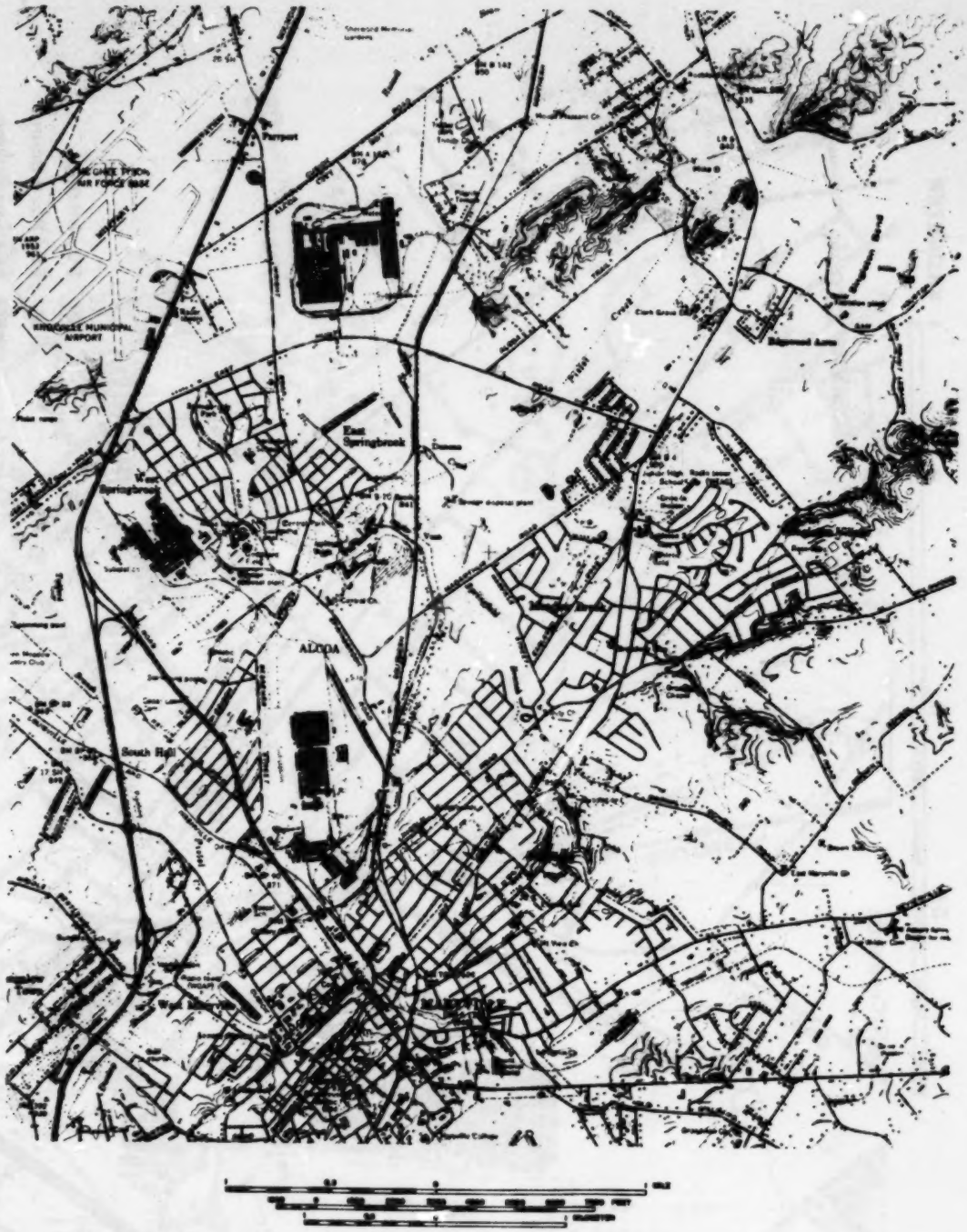

Figure 4-12 Map of Alcoa, Tennessee Area

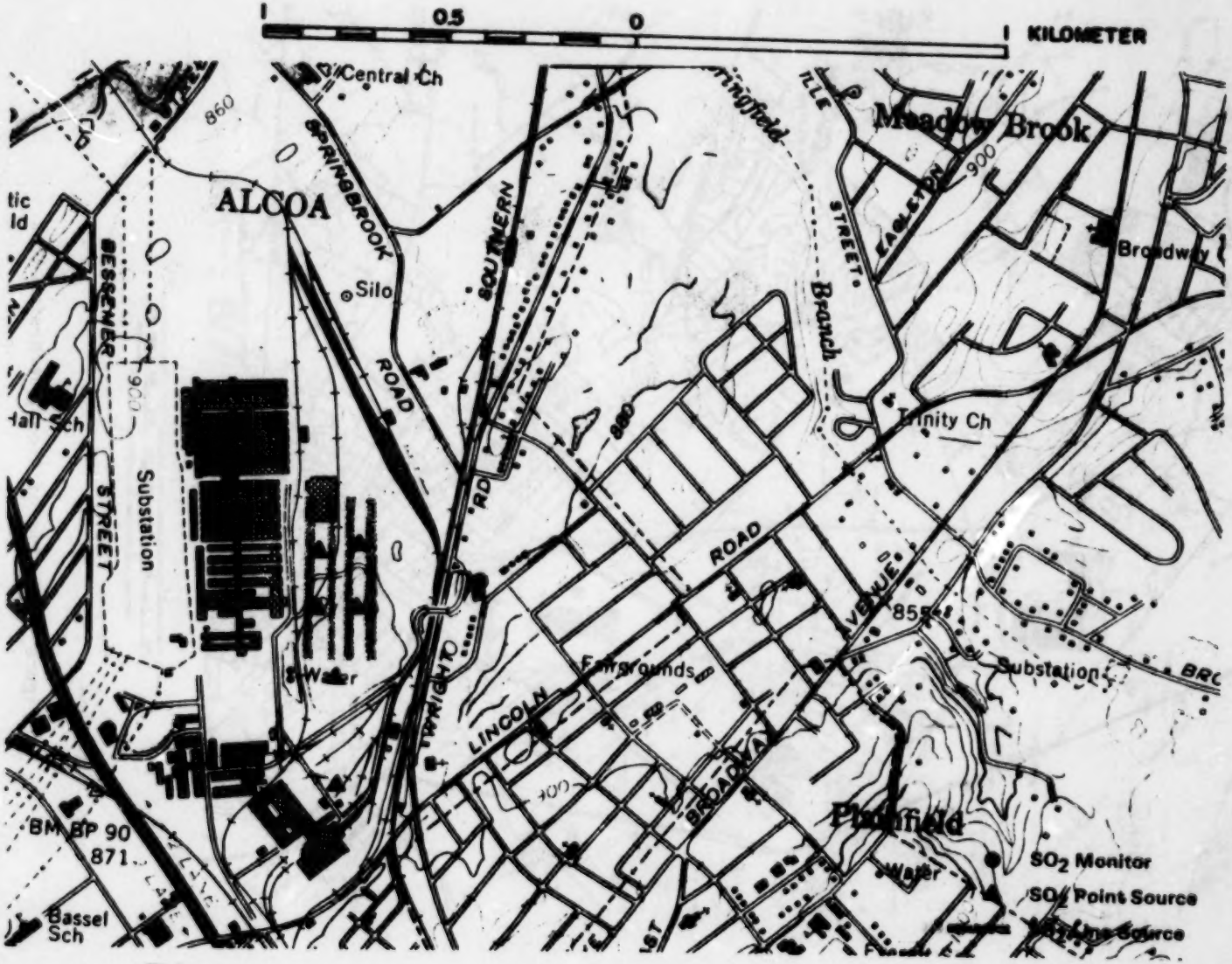

Figure 4-13 Location of the Line and Point Sources Simulated in the BLP Model Verification Study

TABLE 4-2

LINE SOURCE CHARACTERISITICS

Source Name	Height (m)	1976		1977	
		Buoyancy Flux (m^4/s^3)	SO_2 Emission Rate (g/s)	Buoyancy Flux (m^4/s^3)	SO_2 Emission Rate (g/s)
Potroom	19.0	673.5	1.8	849.7	1.5
Potroom	19.0	673.5	1.8	849.7	1.5
Potroom	19.0	673.5	2.4	849.7	2.6
Potroom	19.0	673.5	2.4	849.7	2.6

TABLE 4-3

POINT SOURCE CHARACTERISTICS

Source Name	Height (m)	1976			1977		
		Volume Flux (m^3/s)	Stack Temp (^oK)	SO_2 Rate (g/s)	Volume Flux (m^3/s)	Stack Temp (^oK)	SO_2 Rate (g/s)
Scrubber	11.8	179	383.5	23.4	189	381.2	24.6
Scrubber	11.8	186	383.5	24.5	193	381.2	21.0
Scrubber	22.6	199	372.8	23.9	187	382.2	21.4
Scrubber	22.6	207	367.2	23.7	184	379.7	21.0
Carbon Baking	53.3	41	437.2	6.0	41	437.2	6.0
Carbon Baking	33.5	23	438.8	4.5	23	438.8	4.5
Carbon Baking	35.1	21	476.0	4.5	21	476.0	4.5
Carbon Baking	53.3	30	393.7	2.0	30	393.7	2.0

The four banks of scrubber stacks are each composed of either 16 or 32 small stacks that are tightly grouped together. Because of the efficient hooding in the potrooms, the bulk of the SO_2 emissions are exhausted through the scrubber stacks. The short height of the scrubber stacks ensures that the plumes will be downwashed in the wake of the potrooms.

4.2.3 Air Quality Data

Hourly averaged measurements of SO_2 were taken at two monitors in the vicinity of the plant. One monitor is located at ground level, about 300 meters east of the potroom complex. The other is located on the roof of a building approximately 600 meters southwest of the potrooms. The locations of the two monitors are shown on Figure 4-13.

Model predicted SO_2 concentrations were made for the site 300 meters east of the plant. In general, this monitor was better located to measure maximum plant-related concentrations. The rooftop monitor was used to measure upwind background concentrations. For wind directions from the 180^o sector north to south through west of the potrooms, the measured concentrations at the rooftop site were subtracted from measurements at the eastern ground-level site. For wind directions from the other 180^o sector, the ground-level site was upwind of the plant and the concentrations were set equal to zero. In this manner, hourly averaged plant related SO_2 concentrations were determined for 1976 and 1977 at the monitor 300 meters east of the plant for comparison with model predictions.

4.2.4 Evaluation Results

The meteorological and emissions data for 1976 and 1977 were input to the BLP model to predict hourly SO_2 concentrations at the monitor east of the plant. By comparing these predicted concentrations with the observed concentrations, the accuracy of the model can be evaluated.

The inherent nonsteady nature of the atmosphere and uncertainties in the emissions and air quality data limits the ability to judge

model accuracy on an hour-by-hour basis. Therefore, a commonly used statistical tool is a comparison of the observed and predicted cumulative frequency distributions, especially in the upper percentiles. Figure 4-14 through 4-19 show the observed and predicted distributions for 1-, 3-, and 24-hour averaged concentrations for 1976 and 1977 at the monitor 300 meters east of the potrooms.

The agreement of the highest predicted and observed concentrations is very good. In most cases, the highest predicted concentrations are larger than the highest observed concentrations. As expected, with increasing averaging time, the agreement improves because the shorter term extremes are smoothed. In general, it also appears that the comparisons are better in 1977 than in 1976 with higher concentrations being both predicted and observed.

The corresponding ten highest observed and predicted 1-, 3-, and 24-hour averaged concentraions for 1976 and 1977 are presented in Tables 4-4 through 4-6. The highest 1-hour averaged observations are generally only one half to two-thirds of the highest predicted concentrations. This may be caused by using averaged SO_2 emission rates, since on a short-term basis the emissions have been observed significantly higher.

The agreement of the highest predicted and observed 3-hour averaged concentrations is much better. For 1977, six of the highest observed concentrations and four of the highest predicted concentrations occurred on the same days. These were days 50, 81, 77, and 314. This supports the ability of the model to realistically simulate those events leading to the highest observed concentrations.

The 24-hour averages show an even closer agreement. For both years, the highest predicted concentrations are generally less than 20% larger than the highest observed concentrations. The rate and amount of decrease in concentration from the highest to tenth highest value also agrees well. In 1977, days 50, 81, 77, and 314 appear in both the eight highest observed and predicted concentrations. In other words, half of the eight highest concentrations are predicted and observed on the same days. In view of the uncertainties in emission rate and meteorology, specifically wind direction, this is an important achievement.

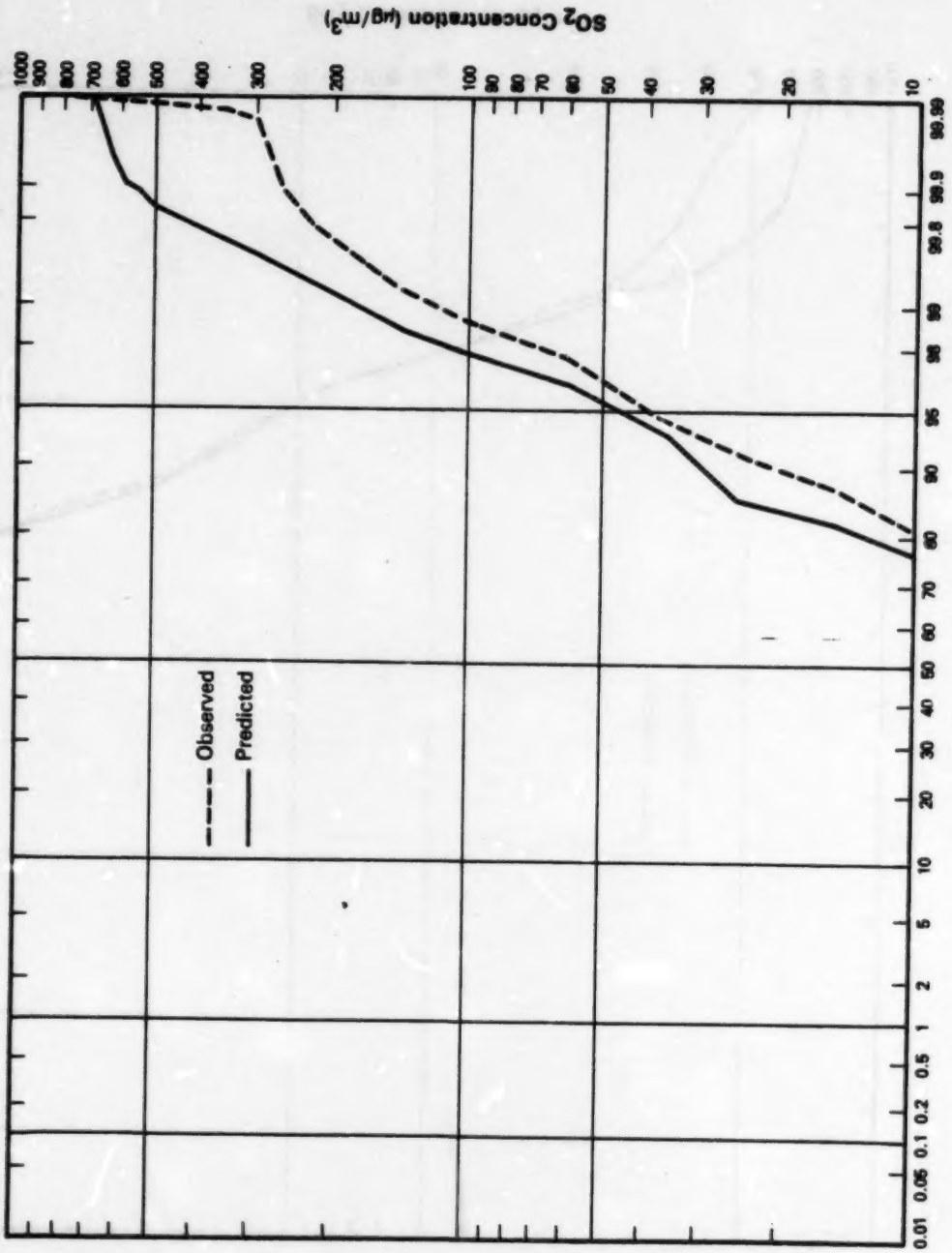

Figure 4-14 Cumulative Frequency Distribution for 1-Hour Averages (1976)

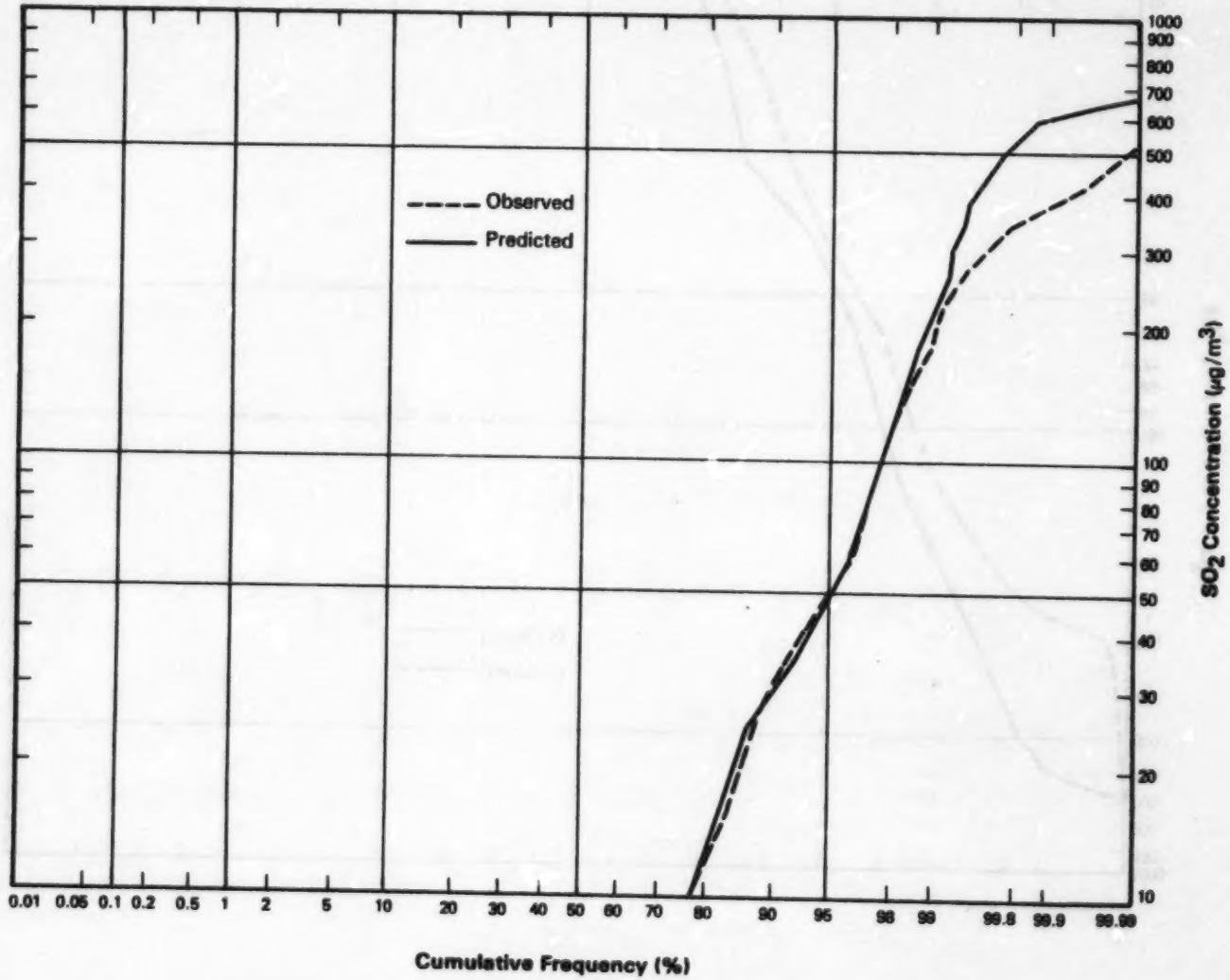

Figure 4-15 Cumulative Frequency Distribution for 1-Hour Averages (1977)

ENVIRONMENTAL RESEARCH & TECHNOLOGY INC

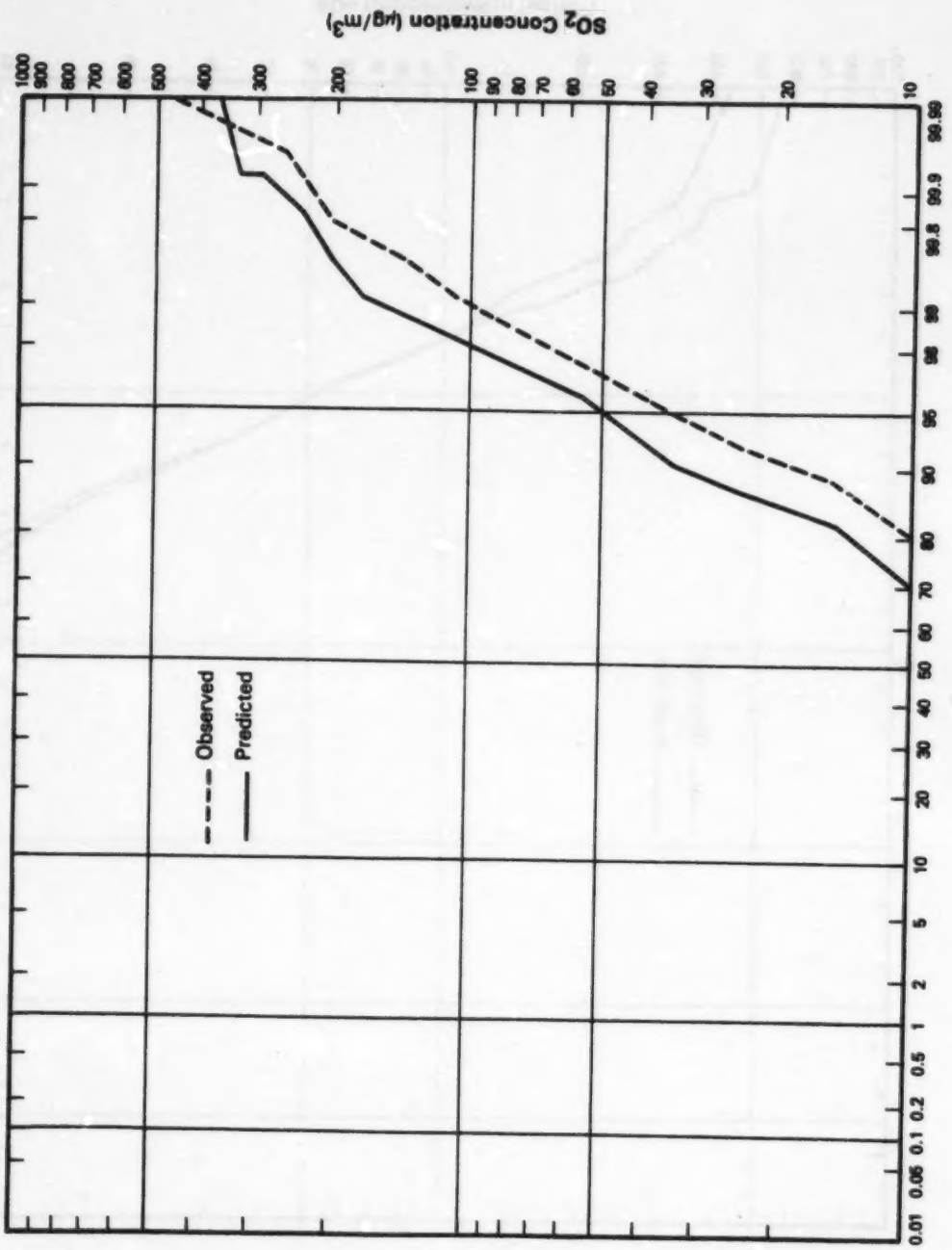

Figure 4-16 Cumulative Frequency Distribution for 3-Hour Averages (1976)

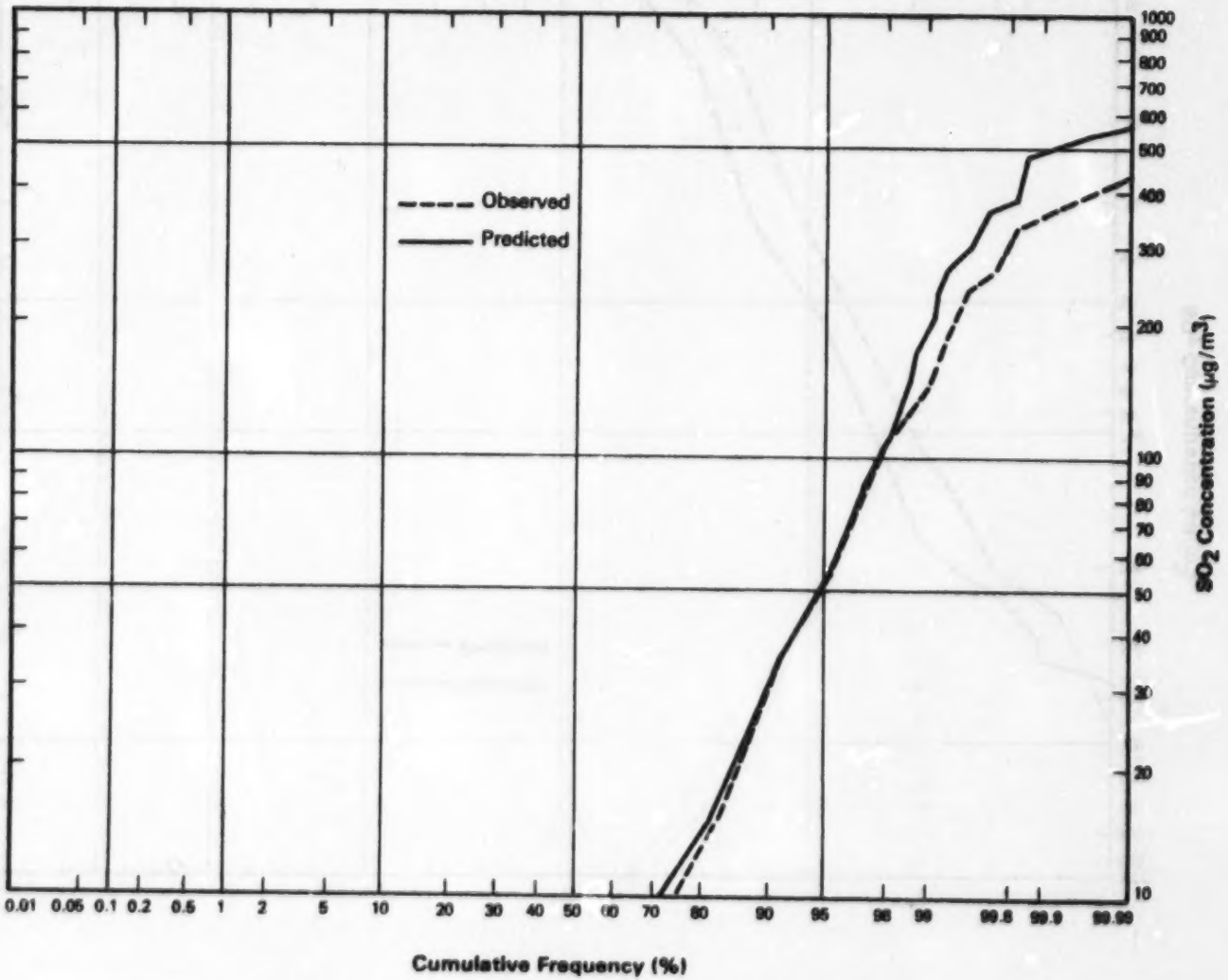

Figure 4-17 Cumulative Frequency Distribution for 3-Hour Averages (1977)

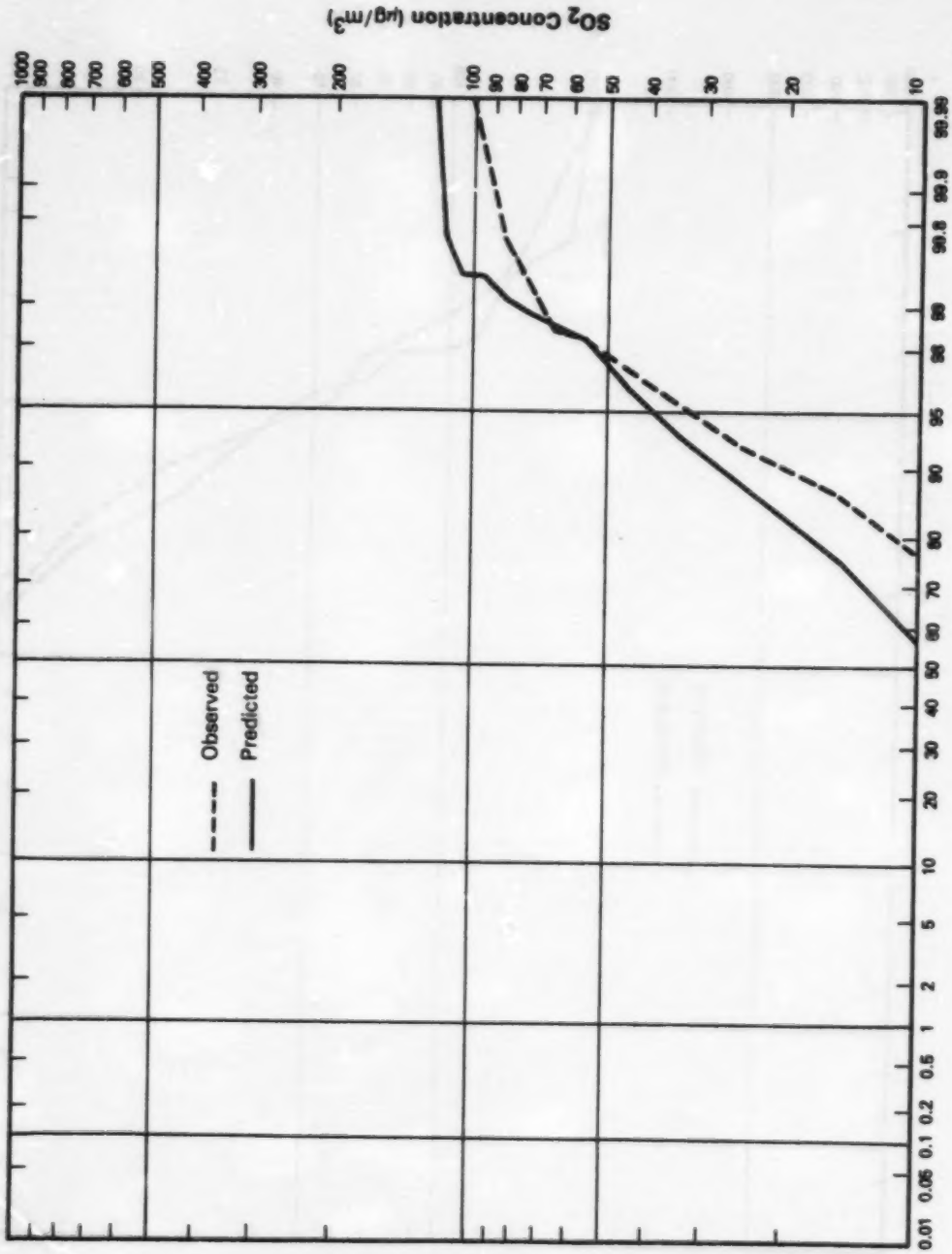

Figure 4-18 Cumulative Frequency Distribution for 24-Hour Averages (1976)

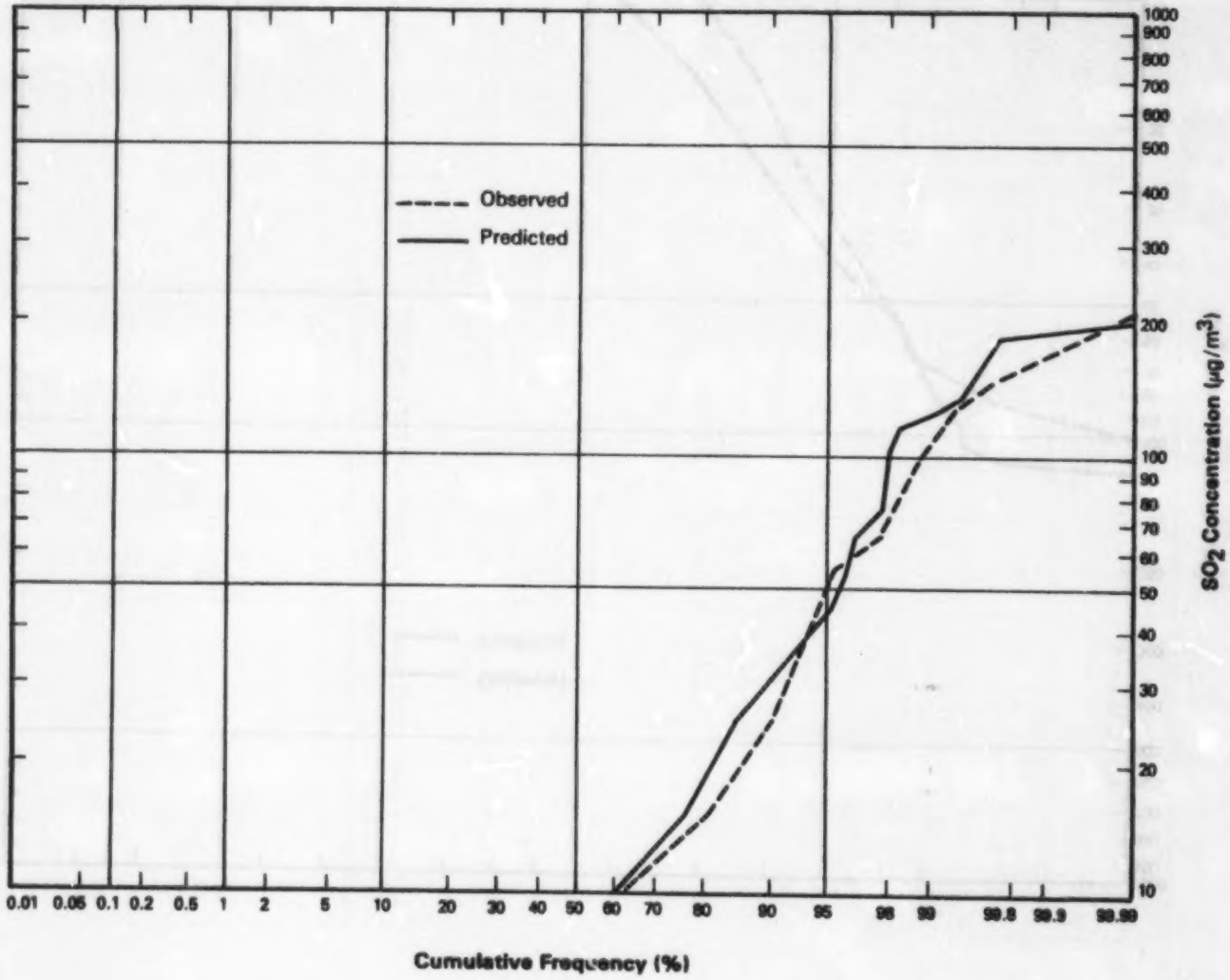

Figure 4-19 Cumulative Frequency Distribution for 24-Hour Averages (1977)

TABLE 4-4

TEN HIGHEST OBSERVED AND PREDICTED CONCENTRATIONS

(1-Hour Average)

	1976					
	Observed			Predicted		
Rank	Day	Hour Ending	SO_2 Concentration ($\mu g/m^3$)	Day	Hour Ending	SO_2 Concentration ($\mu g/m^3$)
1	307	15	779	87	16	684
2	307	13	332	87	9	659
3	307	14	312	87	15	658
4	32	23	305	138	11	652
5	30	9	294	116	20	635
6	283	7	291	25	24	629
7	32	22	286	30	13	606
8	351	17	285	81	15	592
9	8	2	270	116	8	587
10	315	16	263	168	15	555

	1977					
	Observed			Predicted		
Rank	Day	Hour Ending	SO_2 Concentration ($\mu g/m^3$)	Day	Hour Ending	SO_2 Concentration ($\mu g/m^3$)
1	340	8	526	339	10	682
2	340	20	504	95	14	657
3	50	17	484	77	16	651
4	112	8	428	96	12	646
5	81	8	428	81	2	642
6	112	9	400	96	13	622
7	81	9	400	10	6	619
8	343	11	399	55	17	617
9	339	15	398	77	13	616
10	50	16	396	55	16	611

TABLE 4-5

TEN HIGHEST OBSERVED AND PREDICTED CONCENTRATIONS

(3-Hour Average)

	1976					
	Observed			Predicted		
Rank	Day	Hour Ending	SO_2 Concentration ($\mu g/m^3$)	Day	Hour Ending	SO_2 Concentration ($\mu g/m^3$)
1	307	15	474	81	18	368
2	32	24	280	87	18	363
3	351	21	240	3	12	293
4	283	9	235	116	18	256
5	351	18	223	81	12	250
6	315	15	200	61	18	250
7	326	15	194	116	21	249
8	294	15	184	194	15	242
9	295	21	183	76	12	231
10	21	24	179	87	15	231

	1977					
	Observed			Predicted		
Rank	Day	Hour Ending	SO_2 Concentration ($\mu g/m^3$)	Day	Hour Ending	SO_2 Concentration ($\mu g/m^3$)
1	340	9	429	55	18	559
2	50	18	406	10	9	535
3	112	9	340	95	15	529
4	81	9	340	50	15	522
5	340	21	332	95	12	476
6	340	18	282	77	18	397
7	314	6	271	81	3	393
8	314	15	259	96	12	393
9	77	15	259	314	18	379
10	314	18	254	335	12	349

TABLE 4-6

TEN HIGHEST OBSERVED AND PREDICTED CONCENTRATIONS

(24-Hour Average)

Rank	1976			
	Observed		Predicted	
	Day	SO_2 Concentration ($\mu g/m^3$)	Day	SO_2 Concentration ($\mu g/m^3$)
1	351	99	116	121
2	81	80	87	112
3	21	79	81	96
4	326	74	3	88
5	315	73	355	78
6	37	63	76	64
7	312	56	194	60
8	327	52	111	58
9	3	51	53	56
10	294	50	37	56

Rank	1977			
	Observed		Predicted	
	Day	SO_2 Concentration ($\mu g/m^3$)	Day	SO_2 Concentration ($\mu g/m^3$)
1	340	214	10	201
2	314	142	95	185
3	50	121	55	131
4	81	105	96	126
5	112	96	314	123
6	51	93	81	123
7	321	71	50	114
8	77	68	77	103
9	315	68	63	73
10	343	67	335	73

The annual average concentrations are shown in Table 4-7. The agreement, especially in 1977, is excellent.

The horizontal concentration gradients in the nearest few hundred meters of an aluminum reduction plant can be steep. Small changes in wind speed or direction can significantly alter the observations and predictions at a fixed monitoring site making hour-by-hour agreement difficult. This effect can be illustrated by studying the predicted concentration fields on the two days in 1977 with the highest predicted and observed concentrations, days 10 and 340.

Day 10 predicted concentrations are shown in Figure 4-20. The predicted concentration at the monitor is 201 $\mu g/m^3$, less than the maximum observed concentration of 214 $\mu g/m^3$ on day 340. However, only about 100 meters closer to the plant, predicted concentrations are about 300 $\mu g/m^3$. Day 340 predicted concentrations are shown in Figure 4-21. The observed concentrations at the monitoring site is 214 $\mu g/m^3$, but the predicted concentration is only 61 $\mu g/m^3$. However, once again, only 100 meters closer to the plant concentrations greater than 200 $\mu g/m^3$ are predicted. In this case, just a change in wind direction would increase the predicted concentration at the monitor to over 100 $\mu g/m^3$. It is also interesting to note how rapidly the predicted ground-level concentrations decrease with distance. Within about 500 meters, concentrations decrease from about 300 $\mu g/m^3$ to 50 $\mu g/m^3$. This effect was observed during the SF_6 field study and represents the lifting of the initially downwashed buoyant plume.

Not only does the model predict the highest observed concentrations in the vicinity of aluminum reduction plants, but the corresponding meteorology is also in excellent agreement. On both the days with highest observed and predicted concentrations, the associated meteorology was persistent high wind speed (7-10 m/s) neutral stability conditions. This indicates the dispersion processes are probably being correctly simulated.

A linear regression analysis of predicted versus observed concentrations was conducted for 1976 and 1977. One, 3-, and 24-hour averages were compared for the entire year. The resulting correlation coefficients are presented in Table 4-8. Considering the

TABLE 4-7

ANNUAL AVERAGE CONCENTRATIONS ($\mu g/m^3$)

	1976	1977
Observed	8	13
Predicted	13	14

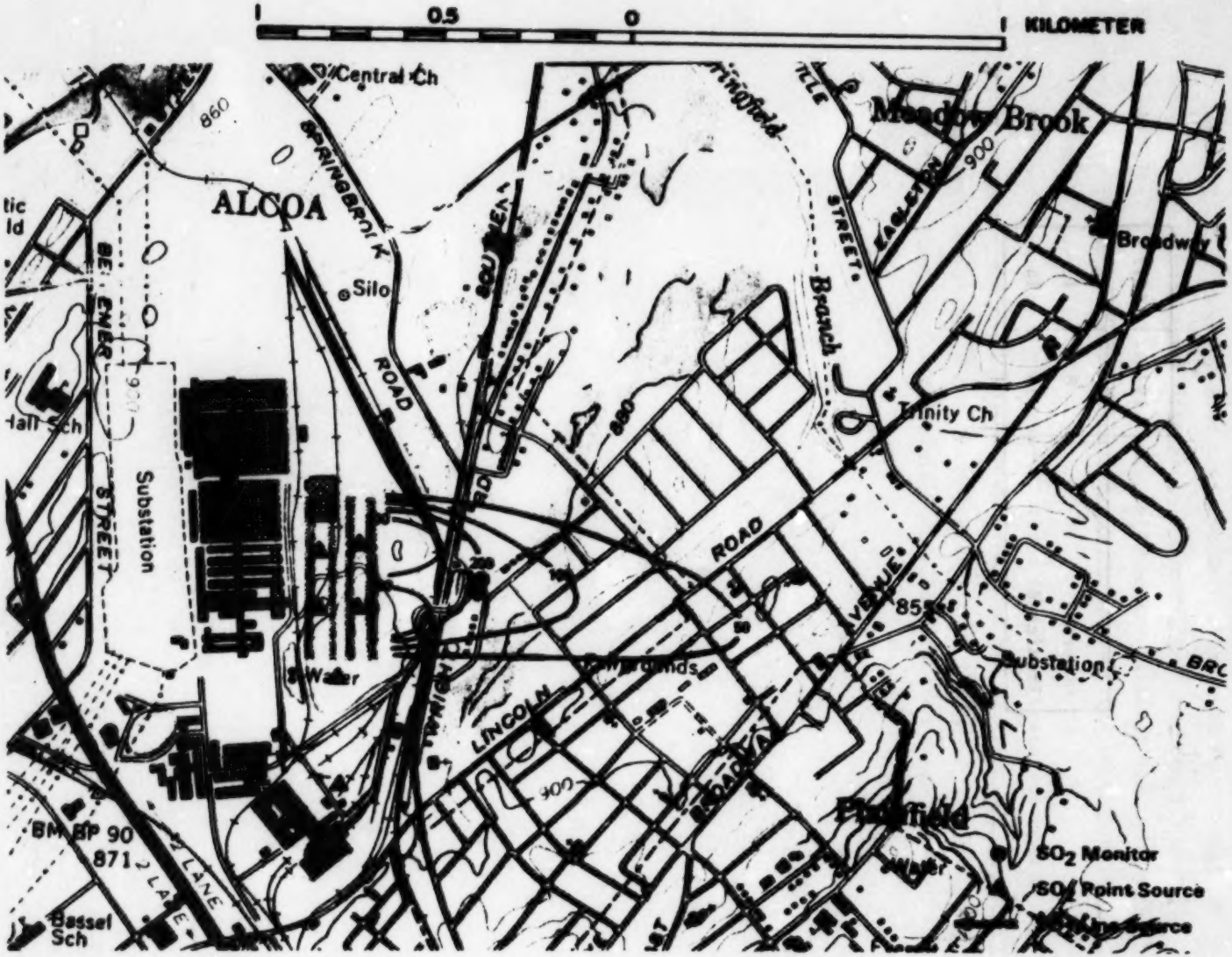

Figure 4-20 Predicted 24-Hour Average SO_2 - Day 10, Year 1977

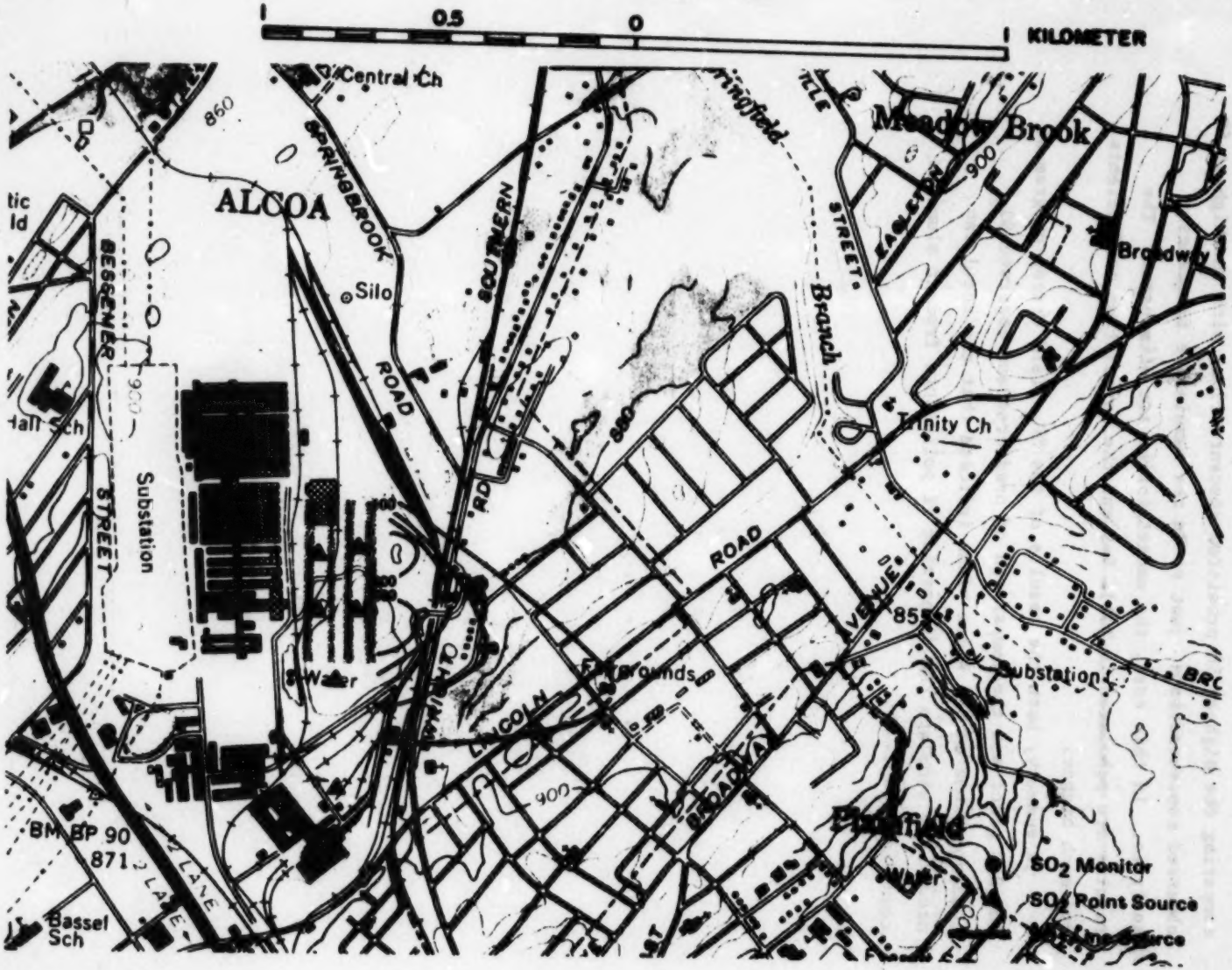

Figure 4-21 Predicted 24-Hour Average - Day 340, Year 1977

ENVIRONMENTAL RESEARCH & TECHNOLOGY INC.

uncertainties involved in comparing hour-by-hour concentrations, the results are fairly good. A second regression analysis was conducted comparing the highest 50 predicted concentrations with the highest 50 observed concentrations, just as in the cumulative frequency analysis. In this case, the uncertainties are eliminated. The results are tabulated in Table 4-9 and the correlation coefficients are much higher.

In summary, both the results of the SF_6 field tracer program at the RMC plant and the comparison of predicted and observed SO_2 concentrations at the Alcoa plant indicate that the model can accurately simulate the dispersion of pollutants from an aluminum reduction plant.

TABLE 4-8

CORRELATION COEFFICIENTS

ALL AVERAGING PERIODS

Year	1-Hour	3-Hour	24-Hour
1976	0.32	0.43	0.61
1977	0.35	0.45	0.59

TABLE 4-9

CORRELATION COEFFICIENTS

TOP 50 AVERAGING PERIODS

Year	1-Hour	3-Hour	24-Hour
1976	0.72	0.93	0.98
1977	0.94	0.98	0.97

5. SUMMARY AND CONCLUSIONS

This report summarizes the research program conducted by ERT to develop and verify an air quality dispersion model to simulate the transport and diffusion of emissions from aluminum reduction plants.

The model development and verification program consisted of four phases.

1) A wind tunnel study of two existing aluminum reduction plants (RMC Patterson Reduction Plant in Arkadelphia, Arkansas and Alcoa Tennessee South Reduction Plant in Alcoa, Tennessee) was performed to evaluate the effects of source size and configuration, wind speed, and wind direction on plume rise and dispersion.
2) An SF_6 field study tracer experiment was conducted at the RMC Patterson Reduction Plant to study the dispersion of the line source (potroom) effluents. Twenty-eight hourly concentration measurements were made at 18 downwind sampling sites at distances from 100 meters to 2,250 meters and one upwind site. On-site meteorological conditions were measured using a tethersonde system.
3) A new air quality dispersion model, the Buoyant Line and Point source (BLP) dispersion model was developed based on the data obtained from the wind tunnel and field experiment programs.
4) The model was verified using the SF_6 tracer study data and two years of SO_2 measurements and nearby airport surface meteorological data at the Alcoa Tennessee South Reduction Plant.

The wind tunnel study results indicate that the line source (potroom) emissions were downwashed at all wind speeds tested. The buoyant line source plume, however, subsequently rose, and under the lighter wind speeds, actually lifted off the ground. The distance to plume lift-off increased with increasing wind speed. The line source plume rise showed a wind direction dependence. The plume rise was

highest for winds parallel to the line source and lowest for perpendicular winds. The plumes from the short point sources also experienced building downwash effects.

The field tracer study results showed the same line source plume downwash and lift-off behavior observed in the wind tunnel. Concentration measurements in the field were made for neutral and unstable conditions with primarily perpendicular winds. Under all wind speeds, the ground-level concentration patterns showed the highest concentration in the near field resulting from downwash of the plume. With the lighter wind speeds, the concentrations decreased rapidly with distance indicating the dominance of the plume rise over vertical plume growth. For the higher wind speeds the buoyant rise of the plume was reduced, and the concentrations decreased more slowly with distance.

The wind tunnel and field experiment data indicated that special modeling techniques needed to be developed to properly simulate the dispersion of the effluents from the multiple low-level buoyant line and point sources. The BLP model was designed to include multiple buoyant line source plume rise enhancement, wind direction line source plume rise dependence, as well as the effects of vertical wind shear and downwash on the plume rise from the line and point sources.

The BLP model was verified by both the SF_6 field tracer data at the RMC plant and the SO_2 measurements at the Alcoa plant. The agreement with the SF_6 line source release measurements were particularly excellent, with the downwash and lift-off effects and plume diffusion accurately simulated. Agreement of model predictions with the two years of SO_2 measurements at the Alcoa plant were also very good. The bulk of the emissions from the Alcoa plant were from the short scrubber stacks, and the importance of downwash and vertical wind speed shear in matching the near field concentrations was demonstrated. Comparison of cumulative frequency distributions and the ten highest predicted and observed concentrations for 1-, 3-, and 24-hour averages showed, even with the uncertainties in emission rates and meteorology, very similar behavior. High wind speed neutral conditions were responsible for both the highest predicted and observed concentrations.

Based on the available data from the wind tunnel, tracer study and SO_2 measurement programs conducted in this project, the BLP model does an excellent job of simulating the dispersion of effluents from typical aluminum reduction plants.

REFERENCES

Anfossi, D., G. Bonino, F. Bossa, and R. Richiardone 1978. Plume Rise from Multiple Sources: A New Model. Atmospheric Environment, 12: 1821-1826.

Briggs, G. A. 1969. Plume Rise. USAEC Critical Review Series, TID-25075, National Technical Information Service.

Briggs, G. A. 1970. Some Recent Analyses of Plume Rise Observations. International Air Poll. Confer., Washington, DC.

Briggs, G. A. 1973. Diffusion Estimates for Small Emissions (Draft). Air Resources Atmospheric Turbulence and Diffusion Laboratory. ATOL No. 79.

Briggs, G. A. 1974. Plume Rise from Multiple Sources. Proceedings of Cooling Tower Environment - 1974. University of Maryland Adult Ed. Center, ERDA Sym. Series.

Briggs, G. A. 1975. Plume Rise Predictions. Lectures on Air Pollution and Environment Impact Analyses. American Meteorological Society, Boston, MA.

Hoydysh, W. G., L. Estrada, and K. Perry 1979. Wind Tunnel Model Study of Plume Dispersion Characteristics from Aluminum Reduction Plants. Environmental Science and Services Corporation (ESSCO), New York. Report No. TR-121.

Huber, A. H. and W. H. Snyder 1976. Building Wake Effects on Short Stack Effluents. Preprints of the AMS Third Symposium on Atmospheric Turbulence Diffusion and Air Quality, Raleigh, NC.

Klauber, G. M. and M. D. Mazaika 1979. Dispersion from Roof Monitors: SF_6 Tracer Study at the Reynolds Metals Patterson Plant. Environmental Measurements, Inc., Arnold, MD.

Murphy, B. L. 1975. Plume Rise from a Row of Chimneys. Presented at the 68th Annual APCA Meeting, Boston, MA, June 15-20.

Schulman, L. L. and J. S. Scire 1980. Buoyant Line and Point Source (BLP) Dispersion Model User's Guide. Document P-7304B. Environmental Research & Technology, Inc., Concord, MA.

Scire, J. S., and L. L. Schulman 1980. Modeling Plume Rise from Low-level Buoyant Line and Point Sources. Presented at the Second Joint AMS/APCA Conference on Applications of Air Pollution Meteorology, New Orleans, LA, March.

Sheih, C. M. 1978. A Puff Pollutant Dispersion Model with Wind Shear and Dynamic Plume Rise. Atmospheric Environment, 12: 1933-1938.

APPENDIX

HOURLY FIELD STUDY SF_6 DATA

APPENDIX

HOURLY FIELD STUDY SF_6 DATA

A minus sign (-) indicates a missing value. A plus sign (+) indicates the concentration exceeded the saturation value of 1,000 ppt. The reported normalized concentration for these hours is a lower bound of the actual value.

SF_6 FIELD EXPERIMENT

Observed $\frac{\chi u}{Q_\ell} \times 10^4$ m^{-1}

(March 18, 1979)

Receptor No.	Hour 12	13	14	15
1	0.6	-	-	0.0
2	-	-	-	-
3	15.2	68.9	-	67.1
4	-	-	80.6	57.0
5	0.5	0.7	4.5	0.0
6	-	-	-	-
7	0.7	0.7	0.5	0.4
8	42.7	12.2	19.6	12.7
9	1.4	2.5	25.7	19.0
10	0.6	0.4	12.1	2.8
11	0.6	17.9	1.0	-
12	1.4	0.0	0.6	0.7
13	-	0.4	0.4	0.3
14	6.8	6.8	18.0	15.6
15	0.8	0.8	10.9	2.0
16	0.0	0.0	0.7	0.5
17	0.4	0.4	1.4	1.1
18	0.9	0.4	0.7	0.5
19	-	-	-	-

SF_6 FIELD EXPERIMENT

Observed $\frac{\chi u}{Q_\ell} \times 10^4$ m^{-1}

(March 20, 1979)

Receptor No.	Hour 10	11	12	13
1	0.3	0.5	0.0	-
2	52.7	84.3	117.8	72.4
3	0.2	0.0	0.0	0.0
4	0.3	0.4	0.4	0.4
5	0.3	0.5	-	0.5
6	7.0	8.0	9.7	0.7
7	9.5	14.3	14.8	6.0
8	0.0	0.4	-	0.4
9	0.3	0.6	0.4	0.6
10	0.2	0.3	0.0	-
11	0.2	0.0	0.0	0.5
12	0.3	0.5	0.6	0.7
13	0.9	1.4	0.6	0.9
14	0.2	-	0.4	0.5
15	-	-	-	-
16	0.0	0.5	0.4	0.5
17	-	-	0.0	0.0
18	0.2	0.4	-	0.0
19	0.3	0.5	0.0	0.4

SF_6 FIELD EXPERIMENT

Observed $\frac{\chi u}{Q_\ell} \times 10^4$ m^{-1}

(March 26, 1979)

Receptor No.	Hour 8	9	10	11
1	0.2	-	-	0.5
2	-	15.5	-	180.5+
3	0.4	0.6	0.5	5.1
4	0.2	0.2	0.2	10.5
5	0.1	0.1	0.2	1.8
6	-	-	0.2	5.3
7	0.2	0.1	0.2	0.3
8	0.2	1.2	2.3	1.2
9	0.1	1.6	0.2	1.6
10	0.2	1.6	0.3	1.6
11	0.1	2.4	0.2	2.4
12	0.2	0.3	0.4	0.3
13	0.1	0.9	0.2	0.4
14	0.0	0.3	0.2	0.3
15	0.2	0.4	0.6	0.4
16	0.2	0.4	0.1	0.4
17	0.2	0.3	0.2	0.3
18	0.0	0.4	0.2	0.4
19	0.0	0.3	0.3	0.4

SF_6 FIELD EXPERIMENT

Observed $\frac{\chi u}{Q_\ell} \times 10^4$ m^{-1}

(March 26, 1979)

Receptor No.	Hour 12	13	14	15
1	0.0	0.5	0.0	0.5
2	239.4+	316.6+	316.6+	320.5+
3	12.1	5.2	13.0	3.8
4	23.2	18.7	-	30.4
5	9.6	-	28.5	44.9
6	34.0	73.8	69.0	122.4
7	0.4	2.8	0.4	0.6
8	1.1	0.6	0.8	0.5
9	5.6	4.6	6.2	-
10	3.5	4.6	9.5	11.7
11	15.6	10.0	-	21.8
12	0.5	1.3	0.0	0.9
13	0.0	0.0	0.3	0.5
14	2.8	-	2.2	1.0
15	2.9	2.9	5.1	-
16	0.7	0.6	0.5	1.2
17	0.0	0.0	0.0	0.7
18	0.0	0.0	0.6	0.0
19	0.0	0.4	0.0	0.4

SF_6 FIELD EXPERIMENT

Observed $\frac{\chi u}{Q_\ell} \times 10^4$ m^{-1}

(March 28, 1979)

Receptor No.	Hour 12	13	14	15
1	0.6	-	0.8	0.3
2	-	-	378.4+	339.8+
3	0.4	3.6	0.6	2.0
4	37.8	25.7	18.2	74.7
5	109.7	79.9	97.2	84.9
6	268.7	205.0	268.7	140.7
7	2.3	1.4	6.1	22.9
8	0.7	0.5	0.6	0.4
9	0.7	2.9	5.6	10.8
10	17.2	13.0	8.2	33.0
11	29.5	21.5	23.5	53.7
12	19.7	-	-	0.0
13	0.0	0.6	0.8	0.0
14	0.0	0.4	0.8	0.4
15	-	-	-	-
16	20.1	10.1	10.8	6.8
17	26.9	0.0	1.9	0.0
18	0.9	0.5	0.6	0.8
19	0.7	0.3	0.0	0.0

SF_6 FIELD EXPERIMENT

Observed $\frac{\chi u}{Q_\ell} \times 10^4$ m^{-1}

(March 29, 1979)

Receptor No.	Hour 10	11	12	13
1	0.0	0.0	0.6	0.5
2	382.9+	359.1+	405.4+	386.1+
3	25.3	25.3	-	27.8
4	-	118.5	111.5	-
5	-	-	46.2	40.2
6	42.1	-	57.6	47.1
7	0.7	-	1.1	84.9
8	0.9	0.6	0.6	-
9	35.2	42.4	24.7	58.7
10	49.8	76.1	50.3	42.5
11	67.0	-	129.7	75.3
12	-	-	-	-
13	0.0	0.6	29.6	0.7
14	4.6	6.4	4.5	-
15	32.5	26.2	19.9	29.0
16	0.6	1.5	1.1	0.7
17	0.7	1.2	0.6	1.4
18	0.8	0.5	0.8	-
19	0.6	0.6	0.6	0.6

SF_6 FIELD EXPERIMENT

Observed $\frac{\chi u}{Q_\ell} \times 10^4 \quad m^{-1}$

(March 29, 1979)

Receptor No.	Hour 14	15	16	17
1	0.0	0.4	0.7	0.5
2	-	-	405.4+	316.6+
3	-	68.9	22.7	-
4	143.8	-	-	109.2
5	36.7	9.8	42.2	0.9
6	-	27.2	-	-
7	-	0.9	1.4	0.5
8	-	4.8	0.5	1.2
9	-	-	-	-
10	45.8	32.8	-	17.1
11	-	-	-	37.4
12	-	-	-	-
13	1.7	1.1	1.6	0.8
14	9.8	31.8	10.9	30.4
15	23.1	12.8	50.3	4.7
16	0.8	0.5	0.5	0.3
17	0.5	0.6	1.5	0.4
18	0.8	0.6	1.3	1.9
19	2.7	1.4	-	1.7

SF_6 FIELD EXPERIMENT

Predicted $\frac{\chi u}{Q_\ell} \times 10^4 \quad m^{-1}$

(March 18, 1979)

Receptor No.	Hour 12	13	14	15
1	0.0	0.0	0.0	0.0
2	258.7	258.0	244.4	204.0
3	63.2	51.1	13.8	22.3
4	84.5	63.1	97.9	47.4
5	0.0	0.0	55.1	2.8
6	46.2	25.0	176.9	105.0
7	0.0	0.0	0.0	0.0
8	11.1	8.1	0.0	0.3
9	1.7	0.4	22.6	3.1
10	0.0	0.0	12.1	0.1
11	0.0	0.0	18.4	0.2
12	0.0	0.0	0.0	0.0
13	0.0	0.0	0.0	0.0
14	5.9	2.1	7.9	3.1
15	0.0	0.0	7.2	0.0
16	0.0	0.0	0.0	0.0
17	0.0	0.0	0.0	0.0
18	0.0	0.0	0.0	0.0
19	0.0	0.0	0.0	0.0

SF_6 FIELD EXPERIMENT

Predicted $\frac{Xu}{Q_\ell} \times 10^4$ m^{-1}

(March 20, 1979)

Receptor No.	Hour 10	11	12	13
1	0.0	0.0	0.0	0.0
2	57.2	8.3	0.0	0.6
3	0.0	0.0	0.0	0.0
4	0.0	0.0	0.0	0.0
5	0.0	0.0	0.0	0.0
6	1.2	0.0	0.0	0.0
7	10.3	3.2	0.0	0.2
8	0.0	0.0	0.0	0.0
9	0.0	0.0	0.0	0.0
10	0.0	0.0	0.0	0.0
11	0.0	0.0	0.0	0.0
12	0.0	0.0	0.0	0.0
13	0.7	0.0	0.0	0.0
14	0.0	0.0	0.0	0.0
15	0.0	0.0	0.0	0.0
16	0.0	0.0	0.0	0.0
17	0.0	0.0	0.0	0.0
18	0.1	0.0	0.0	0.0
19	0.0	0.0	0.0	0.0

SF_6 FIELD EXPERIMENT

Predicted $\frac{\chi u}{Q_\ell} \times 10^4$ m^{-1}

(March 26, 1979)

Receptor No.	Hour 8	9	10	11
1	0.0	0.0	0.0	0.0
2	0.0	5.3	66.2	203.3
3	0.0	0.0	0.0	5.7
4	0.0	0.0	0.0	13.9
5	0.0	0.0	0.0	0.0
6	0.0	0.0	0.0	13.4
7	0.0	0.0	0.0	0.0
8	0.0	0.0	0.0	0.1
9	0.0	0.0	0.0	0.0
10	0.0	0.0	0.0	0.0
11	0.0	0.0	0.0	0.0
12	0.0	0.0	0.0	0.0
13	0.0	0.0	0.0	0.0
14	0.0	0.0	0.0	0.0
15	0.0	0.0	0.0	0.0
16	0.0	0.0	0.0	0.0
17	0.0	0.0	0.0	0.0
18	0.0	0.0	0.0	0.0
19	0.0	0.0	0.0	0.0

SF_6 FIELD EXPERIMENT

Predicted $\frac{\chi u}{Q_\ell} \times 10^4$ m^{-1}

(March 26, 1979)

Receptor No.	Hour 12	13	14	15
1	0.0	0.0	0.0	0.0
2	208.9	273.9	254.1	278.0
3	8.7	0.0	2.7	0.0
4	51.6	104.3	103.4	104.8
5	24.0	90.9	82.1	93.3
6	126.2	178.2	180.4	180.5
7	0.0	0.0	0.0	0.0
8	0.0	0.0	0.0	0.0
9	5.3	4.5	22.5	3.1
10	2.3	23.8	21.9	24.2
11	4.7	41.1	34.0	42.8
12	0.0	0.0	0.0	0.0
13	0.0	0.0	0.0	0.0
14	2.3	0.0	2.2	0.0
15	1.2	13.7	14.5	12.9
16	0.0	1.4	0.0	2.4
17	0.0	0.0	0.0	0.0
18	0.0	0.0	0.0	0.0
19	0.0	0.0	0.0	0.0

SF_6 FIELD EXPERIMENT

Predicted $\frac{\chi u}{Q_L} \times 10^4$ m^{-1}

(March 28, 1979)

Receptor No.	Hour 12	13	14	15
1	0.0	0.0	0.0	0.0
2	286.5	285.0	295.1	268.9
3	0.0	0.0	0.0	0.3
4	133.0	117.0	125.4	117.5
5	122.4	108.2	123.1	101.7
6	207.6	195.0	206.2	190.9
7	0.0	0.0	0.0	0.0
8	0.0	0.0	0.0	0.0
9	7.8	2.6	1.9	18.0
10	43.6	30.7	36.4	32.0
11	66.9	54.1	65.4	49.3
12	0.0	0.0	0.0	0.0
13	0.0	0.0	0.0	0.0
14	0.0	0.0	0.0	0.3
15	27.1	15.6	17.5	22.4
16	2.7	5.1	9.5	0.2
17	0.0	0.0	0.0	0.0
18	0.0	0.0	0.0	0.0
19	0.0	0.0	0.0	0.0

SF_6 FIELD EXPERIMENT

Predicted $\frac{\chi u}{Q_\ell} \times 10^4$ m^{-1}

(March 29, 1979)

Receptor No.	Hour 10	11	12	13
1	0.0	0.0	0.0	0.0
2	275.6	263.6	285.6	276.2
3	1.2	5.4	0.0	0.6
4	140.1	124.6	114.9	137.5
5	122.6	96.0	133.0	122.2
6	212.9	200.7	216.8	210.3
7	0.0	0.0	0.0	0.0
8	0.0	0.0	0.0	0.0
9	37.7	36.9	18.4	31.1
10	48.8	31.8	53.9	47.5
11	66.9	44.3	76.0	66.3
12	0.0	0.0	0.0	0.0
13	0.0	0.0	0.0	0.0
14	1.6	5.2	0.2	0.8
15	35.7	21.5	38.0	34.4
16	0.0	0.0	1.0	0.2
17	0.0	0.0	0.0	0.0
18	0.0	0.0	0.0	0.0
19	0.0	0.0	0.0	0.0

SF_6 FIELD EXPERIMENT

Predicted $\frac{\chi u}{Q_\ell} \times 10^4$ m^{-1}

(March 29, 1979)

Receptor No.	Hour 14	15	16	17
1	0.0	0.0	0.0	0.0
2	269.3	255.7	277.5	248.7
3	3.6	4.6	1.2	10.2
4	133.2	109.5	144.2	102.6
5	109.2	83.0	126.9	65.6
6	208.0	186.9	216.6	181.2
7	0.0	0.0	0.0	0.0
8	0.0	0.0	0.0	0.0
9	40.8	27.3	40.5	24.9
10	40.2	23.3	52.5	15.9
11	54.9	34.7	70.9	23.8
12	0.0	0.0	0.0	0.0
13	0.0	0.0	0.0	0.0
14	4.0	3.8	1.6	6.7
15	28.4	15.4	38.6	9.7
16	0.0	0.0	0.0	0.0
17	0.0	0.0	0.0	0.0
18	0.0	0.0	0.0	0.0
19	0.0	0.0	0.0	0.0